INTERIM REPORT

Demonstration and Performance Assessment of Statistical Methods for UXO Characterization.
Wide Area Assessment: Camp Beale, CA

ESTCP Project MM-0325

AUGUST 2008

John Hathaway
Brent Pulsipher
Pacific Northwest National Laboratory

Barry Roberts
Sean McKenna
Sandia National Laboratory

Environmental Security Technology Certification Program

Report Documentation Page

Form Approved
OMB No. 0704-0188

1. REPORT DATE	2. REPORT TYPE	3. DATES COVERED
26 AUG 2008		**00-00-2008 to 00-00-2008**

4. TITLE AND SUBTITLE	5a. CONTRACT NUMBER
Application of Integrated Visual Sample Plan UXO Design and Analysis Module to the Former Camp Beale for the ESTCP Wide Area Assessment Demonstration	5b. GRANT NUMBER
	5c. PROGRAM ELEMENT NUMBER

6. AUTHOR(S)	5d. PROJECT NUMBER
	5e. TASK NUMBER
	5f. WORK UNIT NUMBER

7. PERFORMING ORGANIZATION NAME(S) AND ADDRESS(ES)	8. PERFORMING ORGANIZATION REPORT NUMBER
Pacific Northwest National Laboratory,902 Battelle Boulevard,Richland,WA,99354	

9. SPONSORING/MONITORING AGENCY NAME(S) AND ADDRESS(ES)	10. SPONSOR/MONITOR'S ACRONYM(S)
	11. SPONSOR/MONITOR'S REPORT NUMBER(S)

12. DISTRIBUTION/AVAILABILITY STATEMENT
Approved for public release; distribution unlimited

13. SUPPLEMENTARY NOTES

14. ABSTRACT

15. SUBJECT TERMS

16. SECURITY CLASSIFICATION OF:			17. LIMITATION OF ABSTRACT	18. NUMBER OF PAGES	19a. NAME OF RESPONSIBLE PERSON
a. REPORT	b. ABSTRACT	c. THIS PAGE			
unclassified	**unclassified**	**unclassified**	**Same as Report (SAR)**	**68**	

Environmental Security Technology Certification Program

ESTCP

Application of Integrated Visual Sample Plan UXO Design and Analysis Module to the Former Camp Beale for the ESTCP Wide Area Assessment Demonstration

ESTCP Project # 200325

Final Report
August 26, 2008

J. Hathaway,[(1)] B. Roberts,[(2)] B. Pulsipher,[(1)] S. McKenna[(2)]
[(1)] Pacific Northwest National Laboratory
[(2)] Sandia National Laboratories

Contents

List of Figures

List of Tables

Acronyms/Abbreviations

ApA	anomalies per acre
ASR	archives search report
DQO	data quality objective
EM	Electromagnetic Induction
ESTCP	Environmental Security Technology Certification Program
HFD	hazardous fragment distance
MFD	maximum fragment distance
PNNL	Pacific Northwest National Laboratory
RMSE	root mean squared error
SNL	Sandia National Laboratories
UXO	unexploded ordinance
VSP	Visual Sample Plan (software)
WAA	Wide Area Assessment (Project)

Executive Summary

The former Camp Beale study area is the final site of the original wide area assessment (WAA) project. This site was selected to demonstrate the WAA technologies on a site with more challenging conditions. These conditions pushed the design team to develop the most adaptive transect design of all the WAA demonstration sites. Also, the analysis required additional steps to evaluate the differences between the survey equipment results and the varied spacing of transects over the site. Along with these challenges, the WAA project at Camp Beale provided an opportunity for PNNL and SNL to demonstrate the use of the fully developed and integrated VSP-UXO modules.

Transect Design

While many different munitions were used in each of these areas, a primary munition-of-interest was used to create the transect design for each of the three colored regions identified in Figure E1. These different areas were defined based on historical information about primary munitions used across the site. The primary munition for the green area is 81-mm mortar rounds, the yellow area focuses on 105-mm projectiles, and the red area focuses on target areas generally used for aerial bombing practice. Separate transect designs and analyses were derived for each of these 3 major areas and the results from each area are presented within this report.

In summary, for the 100-lb bomb area (pink region in Figure E1), a 700-ft target area radius was assumed resulting in a transect spacing of 880 ft. For the 105-mm projectile area, a target area radius and transect spacing of 600 ft and 700 ft, respectively (yellow area in Figure E1) were assumed; for the 81-mm mortar area (green area in Figure E1), a 400-ft target area was assumed resulting in a transect spacing of 450 ft. The geophysical survey team used two different sensor systems which had a 1-m-wide footprint and 2-m-wide footprint. Since it was unclear during the design phase which parts of the 81-mm and 105-mm sites would be covered by each system, the probability of traversal and detection numbers reported in Table E1 were conservatively based on 1-m-wide transect coverage. Because of the open terrain at the north end of the site in the 100-lb bomb region, it was anticipated that those transects in that region would primarily be collected using the 2-m-wide transect system. Thus, the traversal and detection probabilities for the target areas in the north were based on 2-m-wide transects. Table E1 summarizes the transect designs for the entire site.

Table E1. Camp Beale site summary of the combined transect designs for the three munition-specific designs.

SUMMARY OF SAMPLING DESIGN	
Primary Objective of Design	Detect the presence of a target area that has a specified size and shape
Type of Sampling Design	Transect
Selected Sample Area	All
Area of Sample Area	18,261 ac
Shape of Target Area of Concern	Circular
Radii of Target Areas Of Concern	400,600, and 700 ft
Transect Pattern	Parallel
Transect Width	1 and 2 m
Computed Spacing Between Transect Centers	450, 700, and 880 ft
Probability of Traversing and Detecting the Target Area	> 90 percent
Probability of Traversing the Target Area	100 percent for all three target areas
Percent of Site Traversed	0.68 percent
Total Length of Transects	386 km

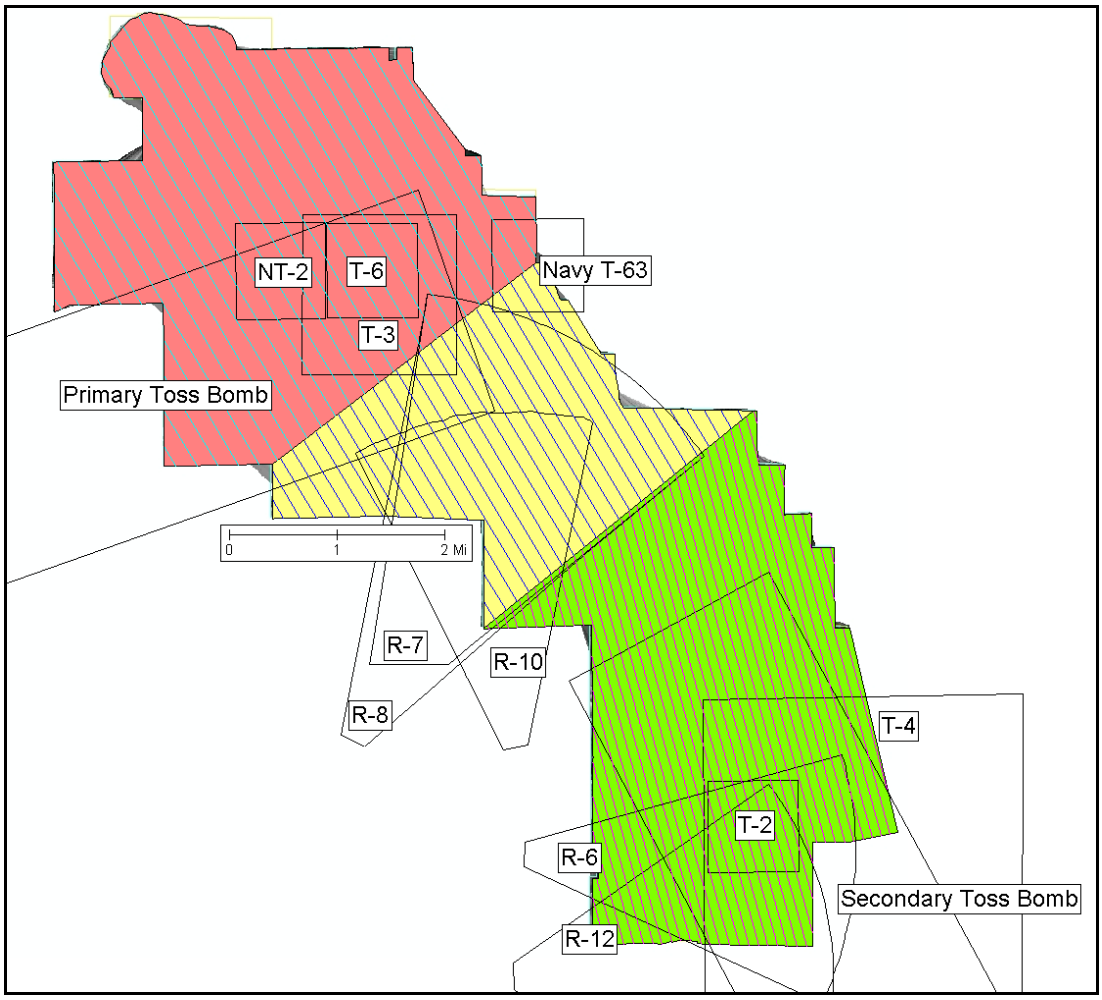

Figure E1. The entire Camp Beale WAA demonstration site showing each of the three finalized transect designs

Target Area Density Estimation and Delineation

Among the WAA study sites, the former Camp Beale site is unique in its use history. Camp Beale site has a complex history of multiple uses (aerial bombing and artillery firing) and multiple overlapping target areas and firing fans (ESTCP 2006). Because of this unique history, a large portion of the site has experienced some level of impact from munitions use. This can be seen in the relatively high anomaly densities observed across the site (Figure E2 and Figure E3). This finding is in contrast to the findings for other WAA study sites (i.e., Pueblo Precision Bombing Range, Victorville, etc.) where distinct isolated target features were superimposed on a relatively low background anomaly density (Hathaway et al. 2006, 2007). The result is that for the Camp Beale WAA site, the highest density areas (red zones in Figure E4 and Figure E5) represent the areas with the greatest impact from past munitions use; however, these areas are not necessarily the only ones that may have experienced munitions use.

The high percentage of high-density areas, along with the overall higher average densities, indicates that the 81-mm mortar analysis area may have experienced heavier and more widespread munitions use than the combined 100-lbs bomb and 105-mm projectile analysis area. The spatial distributions of high-density locations for the two analysis areas also display different patterns. For the 81-mm mortar analysis area, the high-density areas are broken into a series of medium-size patches that are distributed across the analysis area. Typically, these patches are on the order of 300 to 500 acres in size. In contrast, the combined 100-lb bomb and 105-mm projectile analysis area is dominated by a single large high-density area that covers approximately 1500 acres. This is in addition to several smaller high-density areas on the order of 60 acres in size. One of these smaller areas, located to the north of the large high-density area, is associated with a circular terrain target feature as identified in the lidar survey.

The spatial patterns of high anomaly density would suggest munitions use on a larger area, but in a more concentrated fashion in the combined 100-lb bomb and 105-mm projectile analysis area, and in a more distributed fashion in the 81-mm mortar analysis area. Some overlap between these areas also is evident. The patterns of high anomaly density seen in the two analysis areas are not inconsistent with the information available regarding past munitions use at the former Camp Beale WAA site.[1]

For the entire former Camp Beale WAA site, the highest density (red-zone in Figures E4 and E5) area is 4115 acres in size, with an estimated 671,981 magnetic anomalies falling within this area. The total area covered in the geostatistical analysis for this site was 17,877 acres. Therefore, approximately 23 percent of this WAA site is contained within the highest anomaly density (red) zone (Figure E4 and Figure E5). Approximately 58 percent (10,422 acres) of the site has anomaly densities below 50 ApA (the green-zone), and 19 percent of the site (3340 ac) has anomaly densities that are above 50 ApA but below the highest density threshold (the yellow-zone). The total anomaly count exclusive of the red zone is estimated to be 460,906, bringing the estimated total anomaly count for the entire site to well over 1 million. Table E2 provides a summary of these results.

[1] Environmental Security Technology Certification Program (ESTCP). 2006. Wide Area Assessment Pilot Program Demonstration at Former Camp Beale, California. (Unpublished Draft).

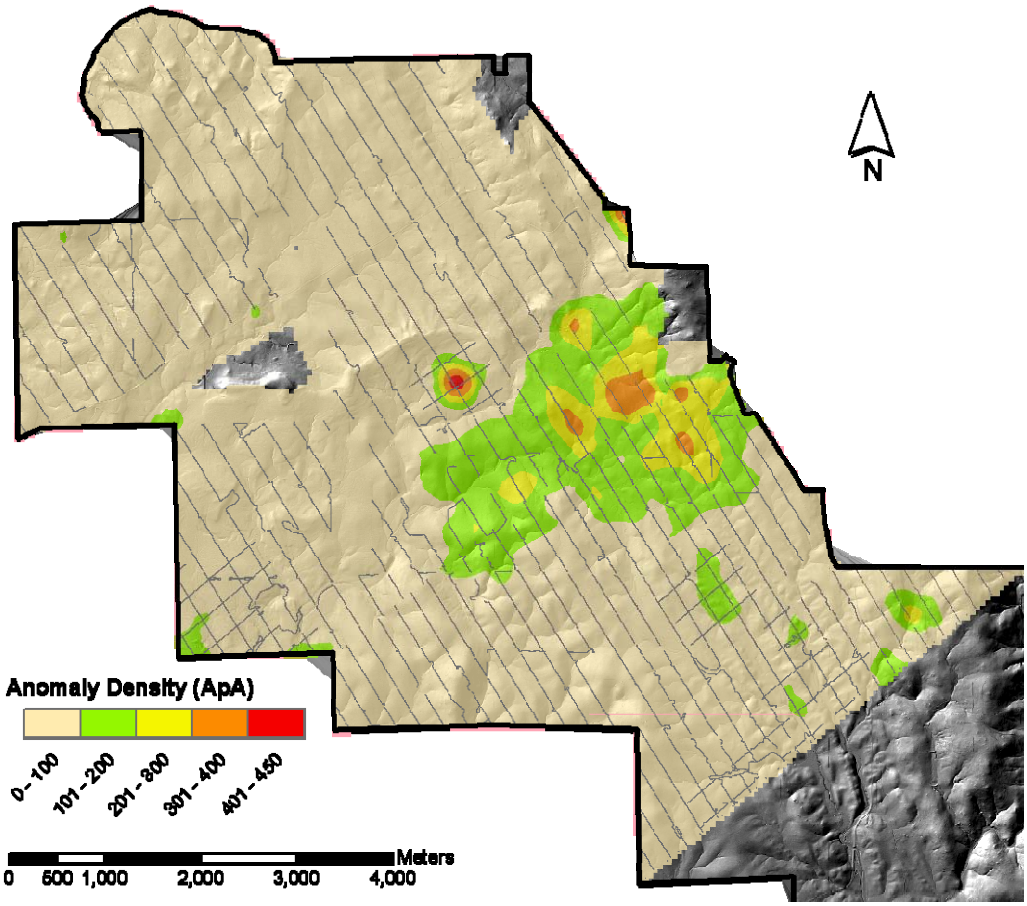

Figure E2. Anomaly density values (ApAs) for the 100-lb bomb and 105-mm projectile combined analysis area. Areas without color shading were not estimated because no observational data were available. Gray-colored lines show transect sample locations.

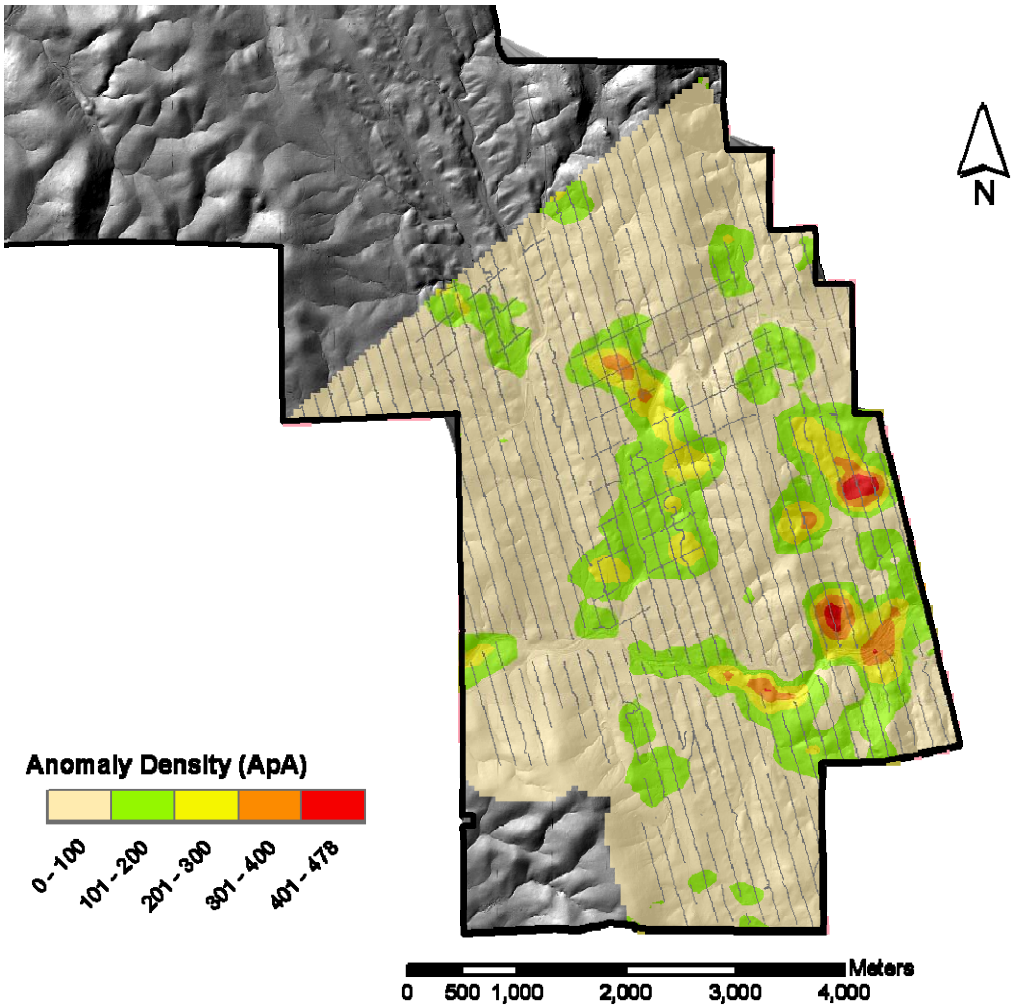

Figure E3. Anomaly density values (ApAs) for the 81-mm mortar analysis area. Areas without color shading were not estimated because no observational data were available. Gray lines show transect sample locations.

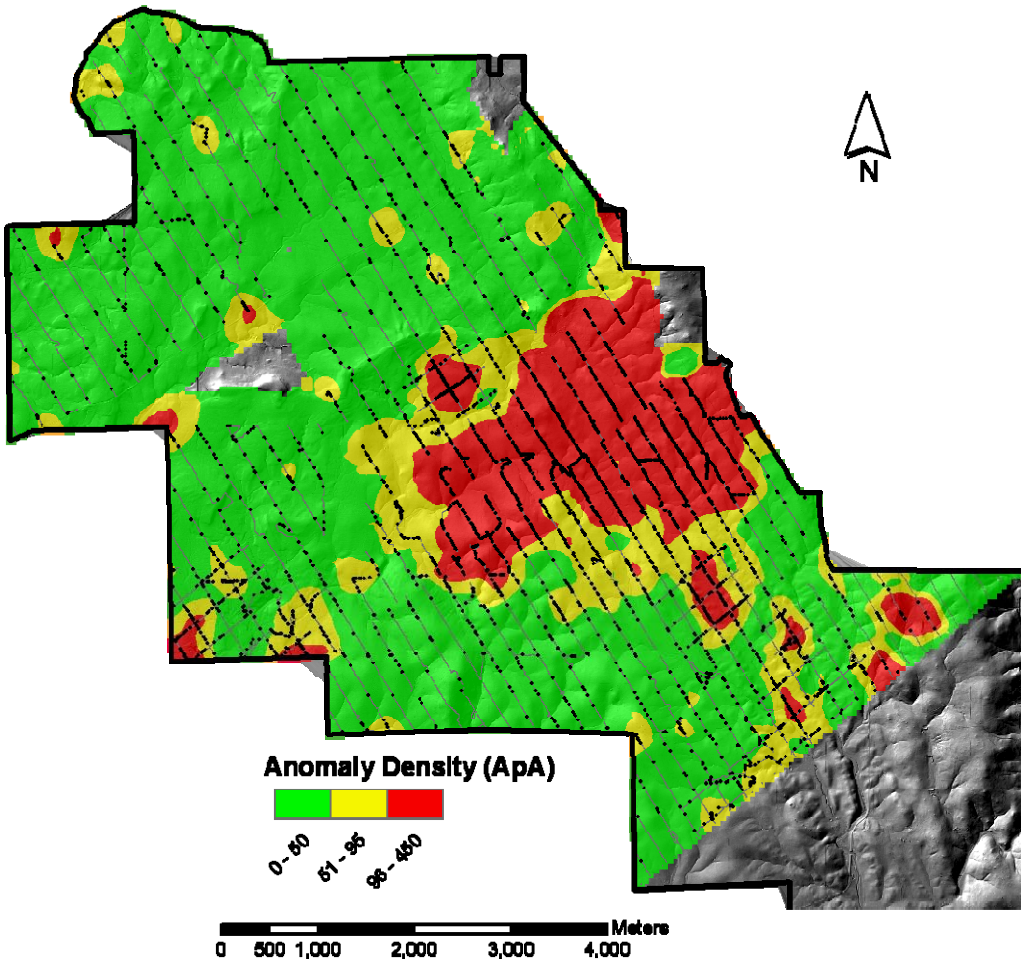

Figure E4. Probable target area delineation for the combined 100-lb bomb and 105-mm projectile analysis area. Color shading indicates the anomaly density range and likelihood of target area location. Red indicates areas most likely to contain target areas; green indicates areas least likely to contain target areas. Yellow regions are transitional zones. Sampling transects and detected anomalies also shown.

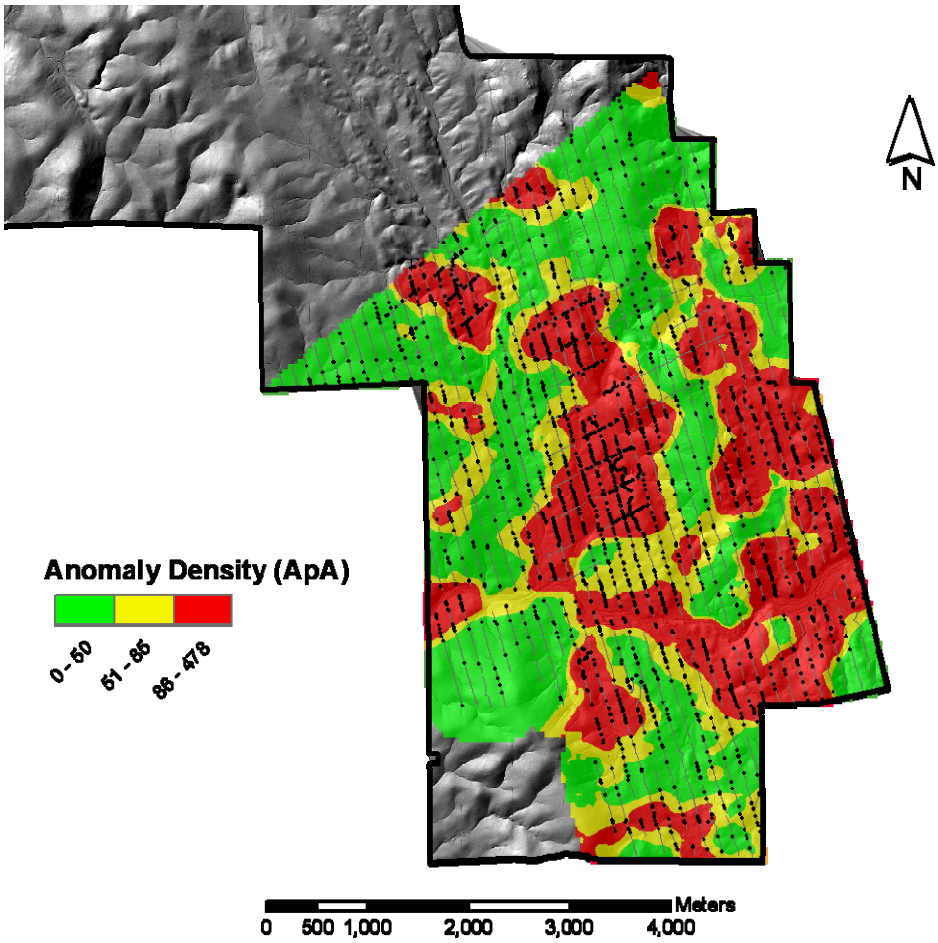

Figure E5. Probable target area delineation for the 81-mm mortar analysis area. Color shading indicates the anomaly density range and likelihood of target area location. Red indicates areas most likely to contain target areas; green indicates areas least likely to contain target areas. Yellow regions are transitional zones. Sampling transects and detected anomalies also are shown.

Table E2. Areas and total anomaly counts for the three color zones of each analysis area.

Analysis Area	Zone (color)	Area (ac)	Total Anomaly Count	Mean Density (ApA)
Combined 100-lb bomb/ 105-mm projectile	Green	7,716	161,683	21.0
	Yellow	1,943	131,274	67.6
	Red	1,825	311,002	170.4
	Total	11,484	603,959	52.6
81-mm mortar	Green	2,706	76,154	28.1
	Yellow	1,397	91,795	65.7
	Red	2,290	360,979	157.6
	Total	6,393	528,928	82.7

1. Introduction

The Environmental Security Technology Certification Program (ESTCP) established several demonstrations of unexploded ordinance (UXO) site characterization technologies under the Wide Area Assessment (WAA) Project. Many of the techniques presented in this report have been documented in reports about previous demonstration sites in Colorado, Ohio, and California (Roberts et al. 2007; Hathaway et al. 2006, 2007).

The WAA project has demonstrated a three-tiered analysis procedure to provide increased certainty of the location of target areas where UXO is most likely to reside. This three-tiered approach, shown in Figure 1, uses the evidence from each system to identify regions of the site either most likely to be target areas that possibly contain UXO or least likely to contain target areas. Pacific Northwest National Laboratory (PNNL) and Sandia National Laboratories (SNL) have developed statistical applications using sparsely spaced, ground-based transects as one component of the bottom tier of the WAA approach.

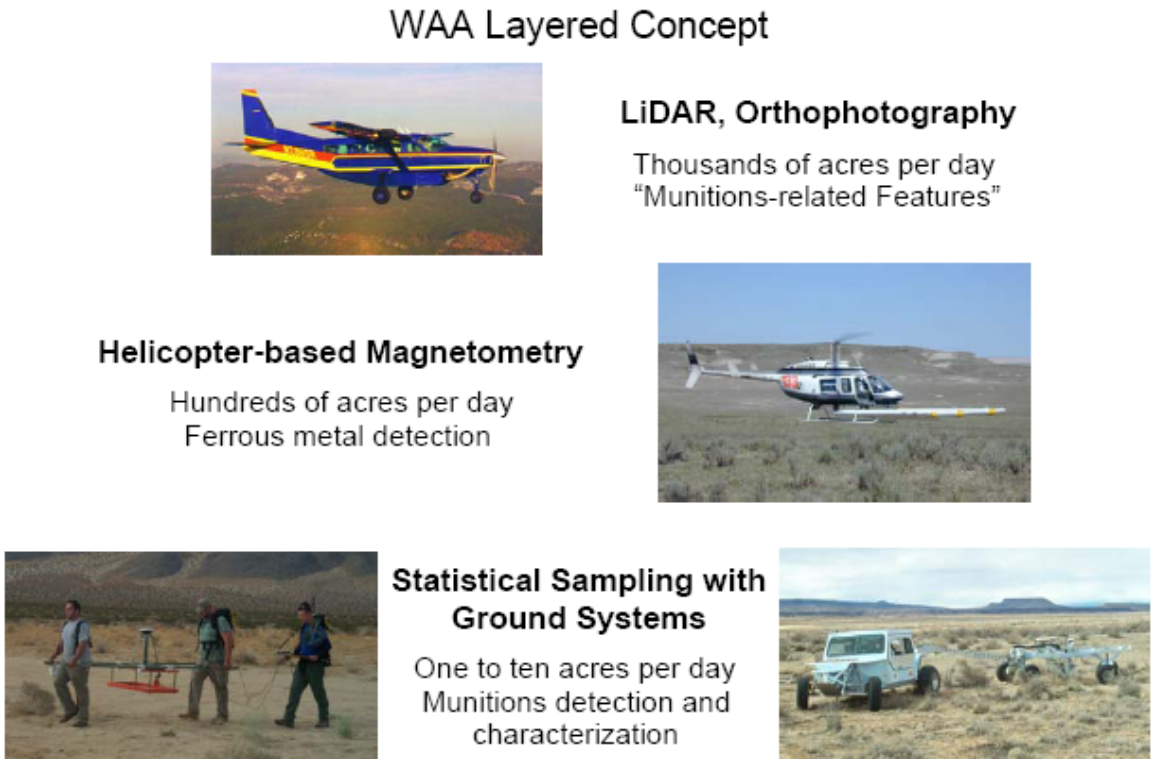

Figure 1. WAA three tier layered approach for identification of target areas.

PNNL and SNL have developed statistical algorithms that use the data quality objective (DQO) structure to create appropriate sparsely spaced transect designs and then analyze these surveyed transects to identify potential target areas within the survey. Target areas are defined as regions of increased geophysical anomaly density relative to the back-

ground density. These transect design tools provide a statistically defensible method that uses transect survey data from a small proportion of the total study area (i.e., 1 to 3 percent) to identify target areas of a specific size, shape, and anomaly density.

Target area density estimates, probability of target area estimates, and density flagging routines are applied after the data are gathered from the established transect design to separate potential target areas from areas that require no further remediation. These tools, combined with the other components of the WAA Project, can be used to correctly and efficiently aid in the investigation of formerly used defense sites.

This report documents the application of these statistically based site characterization tools to the former Camp Beale located in Yuba and Nevada Counties in northern California as part of the ESTCP WAA Project (Figure 2). Specifically, these tools are used to accomplish 1) geophysical transect design to locate potential target areas with agreed upon DQOs, 2) anomaly density estimation across the site using the geophysical data collected along the surveyed transects, and 3) target area boundary delineation.

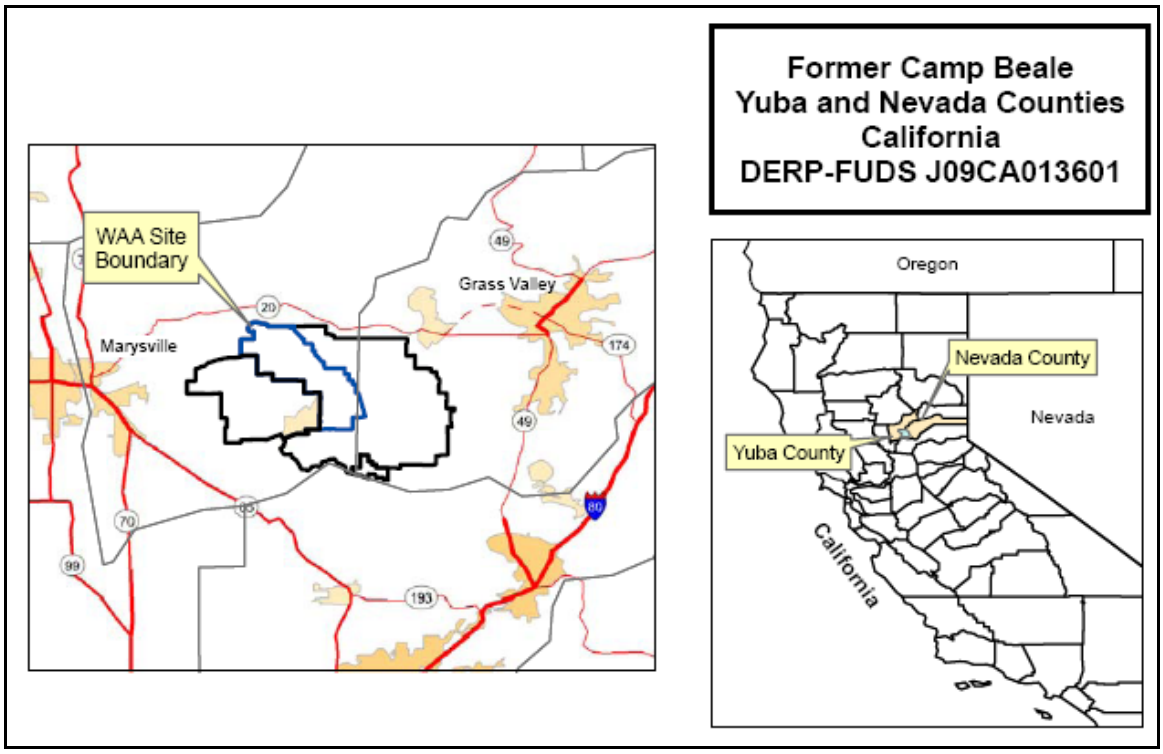

Figure 2. Maps showing the location of the former Camp Beale within the state of California.

1.1. Unique Features of the Former Camp Beale WAA Demonstration Site

Figure 3 shows the 18,000 ac former Camp Beale WAA study area, which is the largest of the ESTCP WAA demonstration sites. In addition to its size, this site has many complicating features that were not encountered at the other demonstration sites. These

complicating features include the terrain, geology, diverse munition use, and multiple deployed ground based systems. Although some helicopter-based surveys were taken in some areas on this site, this report focuses only on data obtained from the ground-based surveys.

Figure 3. Orthophotography of the Former Camp Beale WAA study area. Inset shows a 5X enlargement revealing vegetation and terrain issues.

Terrain

The previous WAA sites had some terrain issues involving steep slopes and vegetation that make geophysical surveys problematic; however, the difficult terrain generally was located on parts of the sites believed to be free from munition use, and these areas were not surveyed as a part of the demonstration. The southern portion of the Camp Beale demonstration area includes steep slopes and significant vegetation (Figure 3) that disallowed the use of the towed-array system. However, this region also was identified as likely to contain high-density target areas containing UXO, so additional man-portable systems were used to survey these regions.

Geology

With the presence of large amounts of magnetic rocks, Camp Beale is similar to the Victorville WAA demonstration site (Hathaway et al. 2006). However, the complications from the geology were addressed in more detail during the deployment stages of the project. With the appropriate ground-based sensors deployed, the geology was less of a factor during the statistical analysis of the transect survey data.

Diverse Munition Use

The WAA study area at Camp Beale included firing ranges that were used for a wide variety of munitions. While the other WAA demonstration sites also had multiple munitions deployed, the munitions generally were different types of aerial bombs. The munitions used at Camp Beale ranged from 60-mm mortar rounds to 1600-lb aerial bombs. This diverse munition use increased the complexity of the site-wide transect designs. It was neither prudent nor cost effective to build a site-wide transect design to identify the smallest target area of interest. However, there was enough evidence that the smaller munitions were primarily used on certain regions of the site to require a small assumed target area for the transect design in these regions. Thus, the transect design was adapted to account for the munitions used within specific portions of the study area.

Multiple Transect Survey Systems

Because of the variety of terrain issues described above, a man-portable electromagnetic induction (EM) system (Harbaugh 2007) was used together with the towed-array EM system (Harbaugh 2006). Photographs of these two systems are shown in Figure 1. While both systems use EM technology, they have different transect footprints. The towed-array system is 2-m wide while the man-portable unit has a 1-m wide footprint. These differences could potentially introduce some discrepancies between the survey results for each system. These potential differences are examined in Section 3.3.

1.2. Improvements to VSP Spawned by Camp Beale Analyses

Although not directly a part of the Camp Beale WAA project, several VSP improvements and enhancements were initiated to be able to handle some of the Camp Beale complexities. These improvements generally dealt with improving the data entry interface, data import and analysis algorithms, and the integration of SNL's geostatistical software.

Many of the original data-handling routines in VSP were developed before the actual course-over-ground data from the WAA demonstration sites were provided to PNNL. The WAA course-over-ground data were much more extensive and were in a slightly different format than anticipated. PNNL developed improved methods to import this data into VSP and updated density calculation algorithms to work more efficiently with the improved detail provided with the course-over-ground files. For a detailed description of

the VSP 5.0 data entry tools, see Hathaway et al. (2008). A full description of the tools available in VSP is also provided in Matzke et al. (2007).

As a part of the WAA demonstration, geostatistical magnetic anomaly density mapping was done using SNL's graphical user interface for the GAM/GAMV and KT3D geostatistical analysis softwares. PNNL and SNL have been integrating VSP and the geostatistical density mapping software while demonstrating the usefulness of these tools on the previous WAA sites. This integration process was mostly completed for the Camp Beale demonstration, and the entire analysis presented in this document is done using the integrated VSP software. Concurrent with the demonstration at Camp Beale, the Visual Sample Plan (VSP)-UXO team developed a two-day instruction course to help transfer this module to contractor use on future sites. This course and the release of VSP 5.0 highlighted the inclusion of many improvements to the usefulness of the UXO modules within VSP.

1.3. Summary

The former Camp Beale study area is the final site of the original WAA project. This site was selected to demonstrate the WAA technologies on a site with more challenging conditions. These conditions pushed the design team to develop the most adaptive transect design of all the WAA demonstration sites. Also, the analysis required additional steps to evaluate the differences between the survey equipment results and the varied spacing of transects over the site. Along with these challenges, the WAA project at Camp Beale provided an opportunity for PNNL and SNL to demonstrate the use of the fully developed and integrated VSP-UXO modules.

This report provides the reasoning behind each of the finalized designs for the Camp Beale WAA project. The transect design sections are followed by a detailed analysis of the surveyed transects. This analysis includes the flagging routines and geostatistical analysis using the VSP software, as well as target area delineations.

2. Former Camp Beale WAA Transect Design

The objective of transect surveying is to identify potential target areas where the anomaly density is higher than background. Transect design development depends on the size, shape, and anomaly density of those target areas of interest. The characteristic size, shape, and anomaly density is dependent on a number of factors but the type of munition used is the primary driver. The overall goal was to develop transect designs that achieved at least a 90 percent probability of traversing and detecting the target areas of interest.

The range locations shown in Figure 4 (black outlines with labels) are the regions where munitions are suspected to have been used. Table 1 lists each of these ranges and the identified munition information that was provided. Based on historical data from the archives search report (ASR) used in conjunction with recently obtained lidar and orthophotography data for Camp Beale, the site was divided into three munition-specific areas.

While many different munitions were used in each of these areas, a primary munition-of-interest was used to create the transect design for each of the three colored regions identified in Figure 4. These different areas were grouped based on three different primary munitions-of-interest. The primary munition for the green area is 81-mm mortar rounds, the yellow area focuses on 105-mm projectiles, and the red area focuses on target areas generally used for aerial bombing practice. Separate transect designs and analyses were derived for each of these 3 major areas and the results from each area are presented within this report. For a more detailed description of how to use the munitions of interest to develop proper transects designs, see Hathaway et al. (2008).

The technical paper "Methodologies for Calculating Primary Fragment Characteristics" known as TP-16 (DDESB 2003) was used to derive the assumed target sizes and areas for each of the three colored regions in Figure 4. The paper examines the fragmentation patterns of many different munitions and details different fragment throw distances associated with each munition. The two primary distances reported are the hazardous fragment distance (HFD) and the maximum fragment distance (MFD). Often there is a large gap between these two values for each munition, and the final assumed target area dimensions are derived using a value that lies between HFD and MFD.

Table 1. Summary of the ASR identified ranges of interest within the WAA boundaries of the Camp Beale study area.

Range	Range Type	Munitions Items Used
Target 2	Demolition bombing	High-explosive charges up to 250 lb; some information is missing
Night Target 2	Bombing	No information found
Target 3	Bombing	Live bomb releases for Shoran training, M38A1, 100-lb bomb
Target 4	Bombing	Proposed target; apparently not used. No information found about munitions used.
Target 6	Bombing Range	Live bomb releases for Shoran training
Navy Target T-63	Bombing target	Mark 76 Navy 25-lb practice bombs; possibly 250- or 500-lb practice bomb
Primary Navy Toss Bomb Target	Bombing target	No information found
Range 7	Ground range	57-mm recoiless rifle; 60-mm mortar, 50-caliber shape charges
Range 8	Ground range	57-mm recoiless rifle; 60-mm mortar, 50-caliber shape charges
Range 10	Ground range	Shape charges
Proposed Secondary Navy Toss Bomb	Bombing target	No information found
Range 6	Bombing, ground range	M38A1 practice bomb, fuse cap from 100-lb bomb; some information
Range 12	Ground range	No information found

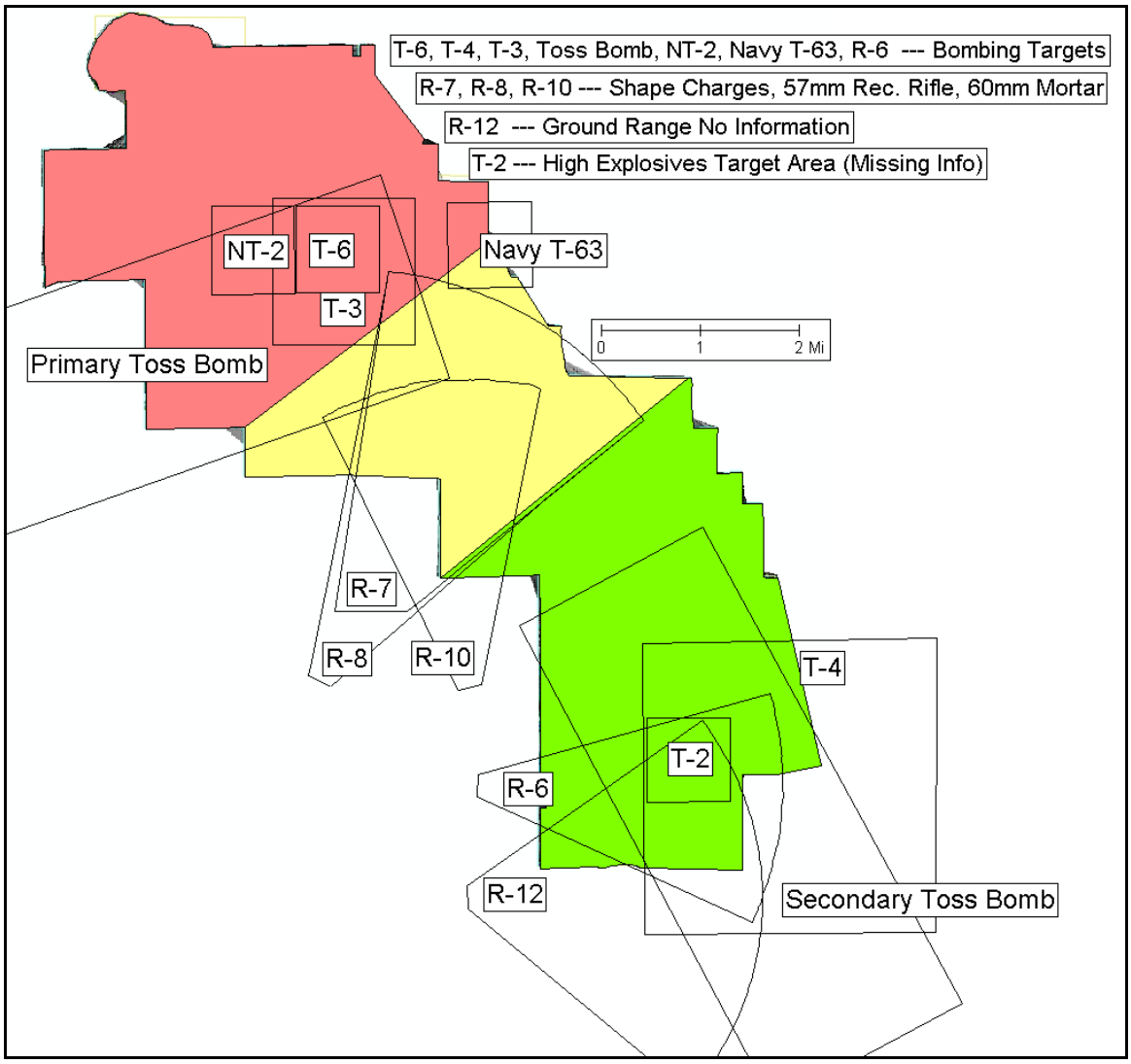

Figure 4. Camp Beale WAA study area divided into three munition-specific regions. The red region was primarily used for aerial bombing, the yellow region is believed to contain target areas for 105-mm projectiles, and the green region contains target areas for 81-mm mortars.

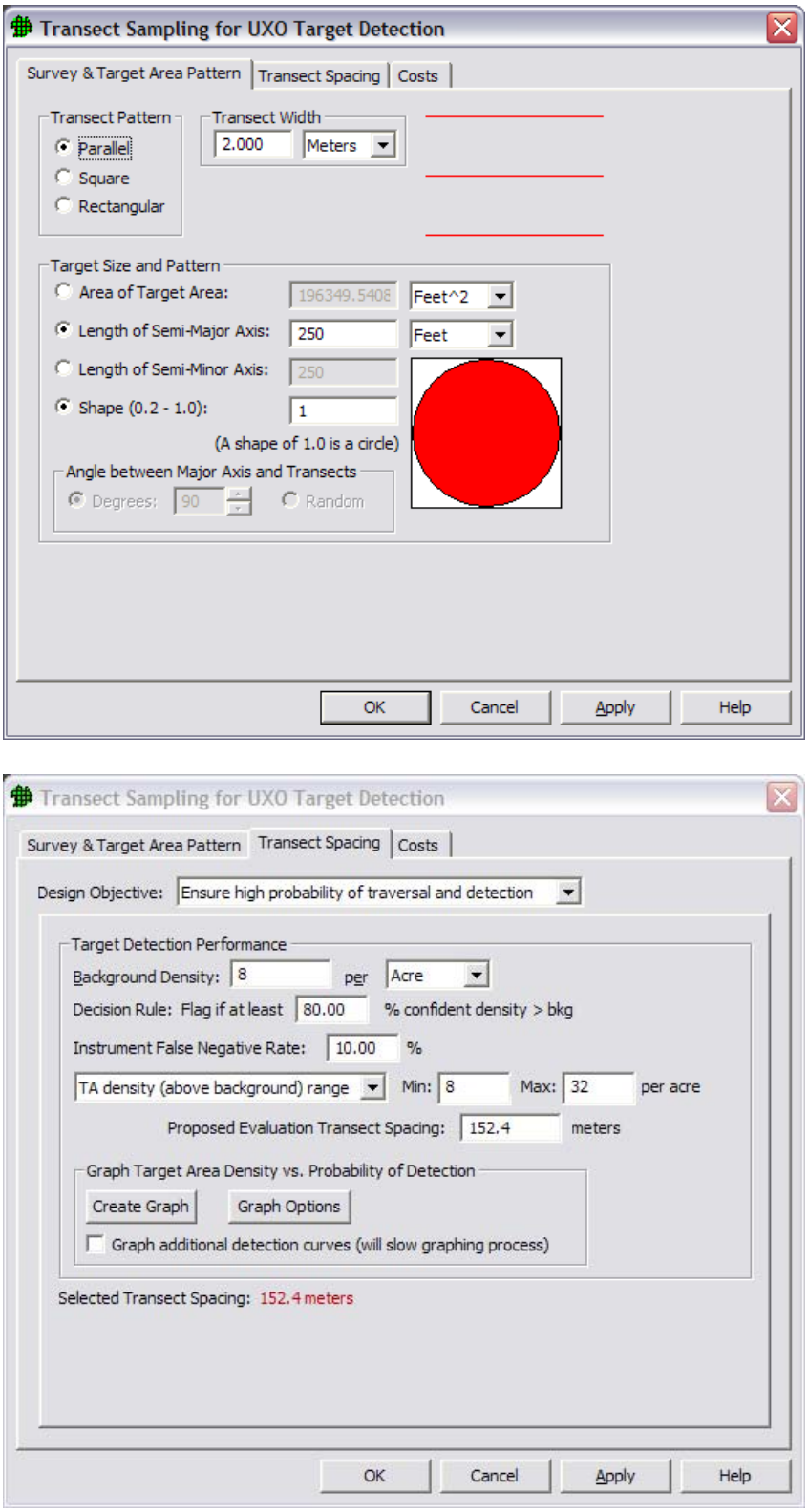

Figure 5. The transect design dialog in VSP allows the user to input transect pattern, width, and target area size, shape, and orientation (top). Probability of detection curves can be displayed based on inputs and site assumptions (bottom).

2.1. 100-lb Aerial Bombing Region

In the 100-lb aerial bombing region, five ranges were identified as potential munitions use regions during the review of the ASR. These five ranges are shown in Figure 6 (red outlines with labels). The yellow outlines identify the regions where man-made features were identified in the orthophotography and lidar. The lidar identified many craters resulting from detonation of high-explosive bombs within the 100-lb bomb region. The lidar and orthophotography also identified that this terrain could be traversed by the towed-array system which has a 2-m-wide transect footprint.

There were multiple aerial bombs listed in the TP-16 report (DDESB 2003). Based on information from the report, the smallest fragmentation range from a 100-lb GP MK 1 bomb had a hazardous fragment distance (HFD) of 200 ft and a maximum fragment distance (MFD) of 1863 ft. The other 100-lb bomb and two other 250-lb bombs identified in the report had an approximate HFD of 500 ft and an MFD of 2100 ft. Using these numbers as a reference, a circular target area (high anomaly density area) with a radius of 700 ft was assumed to be characteristic of a 100-lb bomb munition use and this was used to establish the transect design. The assumed circular target area provided a conservative representation of target areas resulting from bombs that were 100 lb or larger.

For the transect design, a high probability of traversing and flagging a 100-lb bombing target area was desired. Figure 7 shows the probability of traversing and detecting a 700-ft radius target area as a function of the spacing between transects. The three colored lines show the sensitivity of the detection probabilities based on an average target area density of 40 anomalies per acre (ApA), 80 ApA, and 160 ApA above a background density of 45 ApA. The assumed background level of 45 ApA and density above background of 80 ApA were selected based on observations at previous WAA sites (Hathaway et al. 2006, 2007). The input values for the performance curves in Figure 7 are shown in Table 2.

The selected final transect spacing of 880 ft shown in Figure 6 has an approximately 98 percent chance of traversing and detecting any 700-ft radius target area having a bivariate normal geophysical anomaly density distribution with an average density of 80 ApA above the background density of 45 ApA. This assumes that 2-m wide transects are gathered, the anomaly detection false negative rate is zero, and the flagged windows have at least a 95 percent confidence of being greater than background.

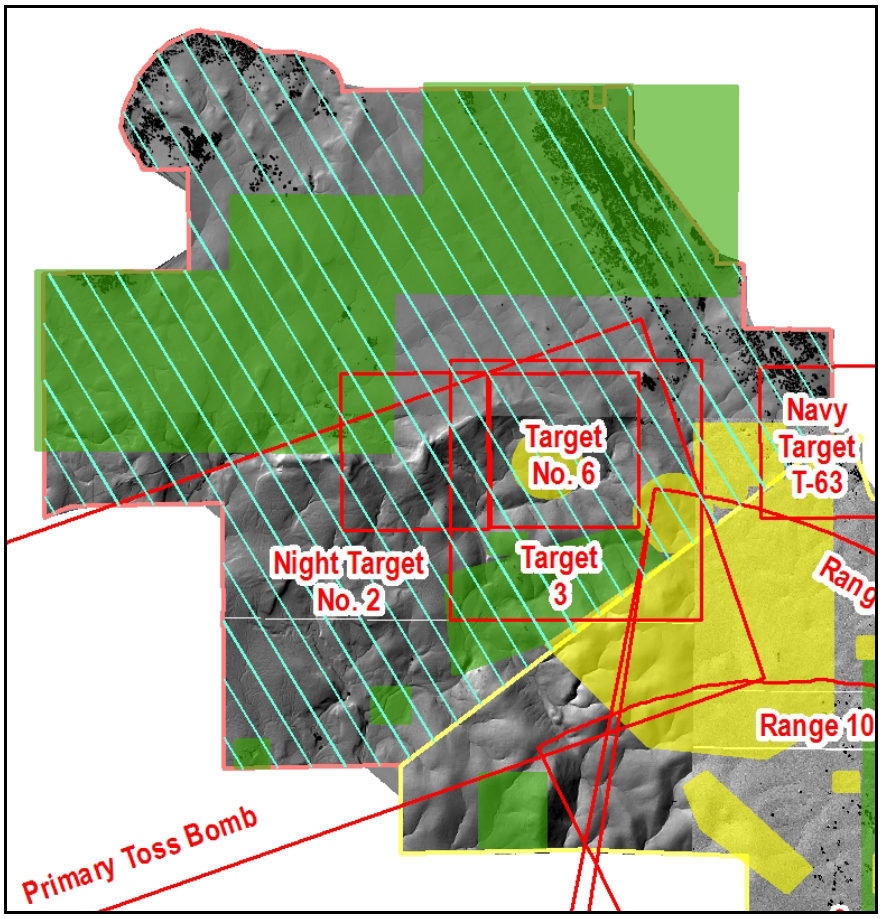

Figure 6. The 100-lb bomb transect design (blue lines) overlaid on a shaded relief of the lidar data for the northern area of Camp Beale. The five historical ranges are outlined in red and labeled. The yellow regions are those areas that show munition-related features based on the lidar data and the green regions show man made features that may be munitions related.

Table 2. The required traversal and detection inputs for the VSP calculations and the respective values used for this design.

VSP Inputs	Design Value
Transect Width	2 m
Transect Pattern	Parallel
Length of Semi-Major Axis	700 ft
Shape	Circular
Background Density	45 ApA
Decision Rule	95 percent
Instrument False Negative Rate	0
Target Area Density Above Background	40/80/160 ApA
Density Distribution	Bivariate Normal Density
Average Target Area Density Input as	Target Average
Minimum Precision/Maximum Error	0.1/0.05

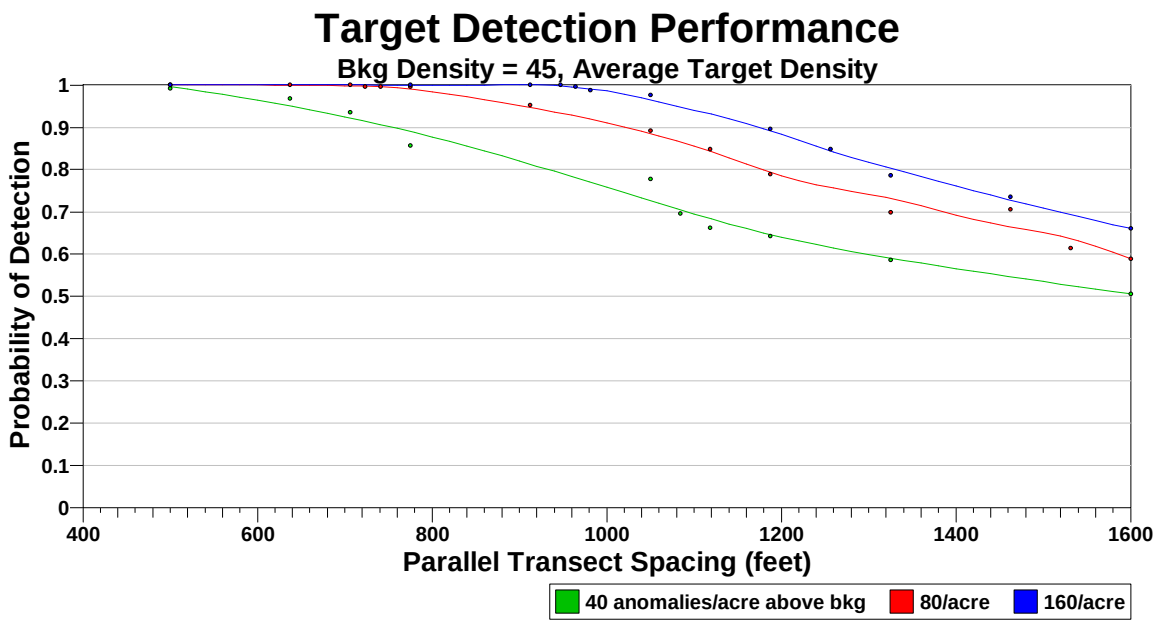

Figure 7. Power curves for the 700-ft radius target area based on 100-lb bombs as a function of transect spacing. Each colored line represents a different density of the target area as labeled. The transect spacing of 880 ft was selected based on this graph.

2.2. 105-mm Projectile Region

There are five ranges that lie within the 105-mm-projectile region (yellow portion of Figure 4). The T-3 and Navy T-63 ranges primarily lie to the north in the 100-lb bomb region. Three ranges (R-10, R-7, and R-8) were identified as potential munition-use regions that directly impacted this region. In addition, the yellow outlines identify the regions where man-made features were identified in the orthophotography and lidar. In the planning stages, it was unclear which of the two survey systems would cover this area because of the terrain. Because of this issue, for the transect design in this region, a 1-m-wide geophysical sensor footprint was assumed.

While the three identified ranges that impacted this region do not include 105-mm projectile use, the ASR did identify that 105-mm and 155-mm projectiles were used in this region. The HFD and MFD of the smaller 105-mm projectile documented in the TP-16 report are 341 ft and 1939 ft, respectively. Both the HFD and MFD for the 105-mm projectiles are about the same as those for the 100-lb bomb region (DDESB 2003). However, the general belief that the target areas for these munitions would tend to be smaller than the target areas for 100-lb bombs suggested a smaller target area would be appropriate. Thus, it may be reasonable to assume a target area with a 600-ft radius.

The target detection performance curves shown in Figure 8 show the probability of traversing and detecting a 600-ft radius target area as a function of the transect spacing. The three colored lines show the sensitivity of the detection probabilities based on an average target area density of 40 ApA, 80 ApA, and 160 ApA above a background

density of 45 ApA. The input values used to create the performance curves in Figure 8 are shown in Table 3.

The final transect spacing of 700 ft, shown in Figure 9, has an approximately 93 percent chance of traversing and detecting any 600-ft radius target area having a bivariate normal distribution with an average density of 80 ApA above the background density of 45 ApA. This assumes that 1-m wide transects are gathered, the false negative rate is zero, and the flagged windows have at least a 95 percent confidence of being greater than background.

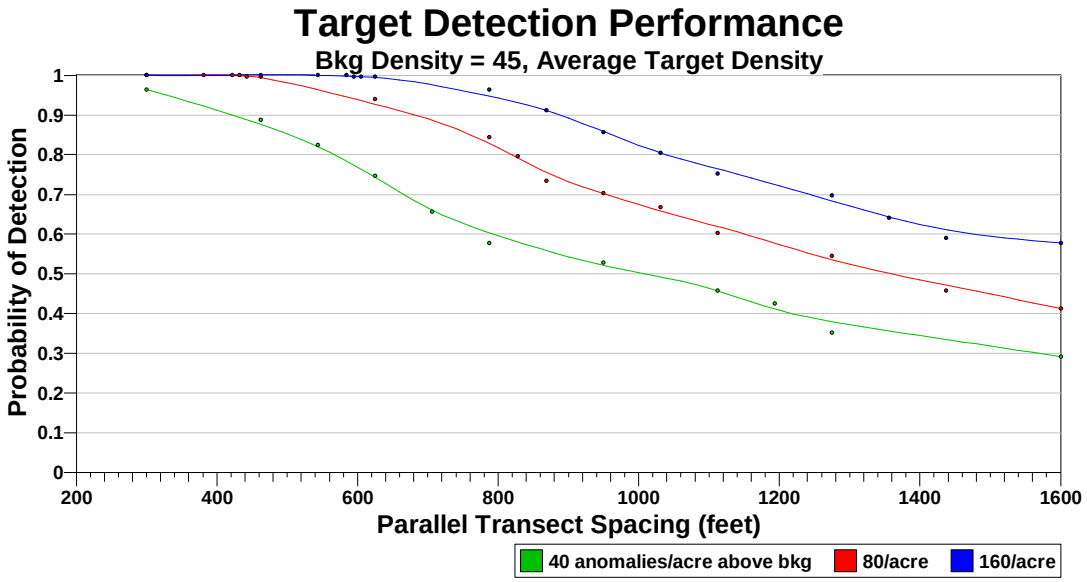

Figure 8. Power curves for the 600-ft radius target area based on the 105-mm projectiles as a function of transect spacing. Each colored line represents a different density of the target area as labeled. The transect spacing of 700 ft was selected based on this graph.

Table 3. The required traversal and detection inputs for the VSP calculations and the respective values used for this design.

VSP Inputs	Design Value
Transect Width	1 m
Transect Pattern	Parallel
Length of Semi-Major Axis	600 ft
Shape	Circular
Background Density	45 ApA
Decision Rule	95 percent
Instrument False Negative Rate	0
Target Area Density Above Background	40/80/160 ApA
Density Distribution	Bivariate Normal Density
Average Target Area Density Input as	Target Average
Minimum Precision/Maximum Error	0.1/0.05

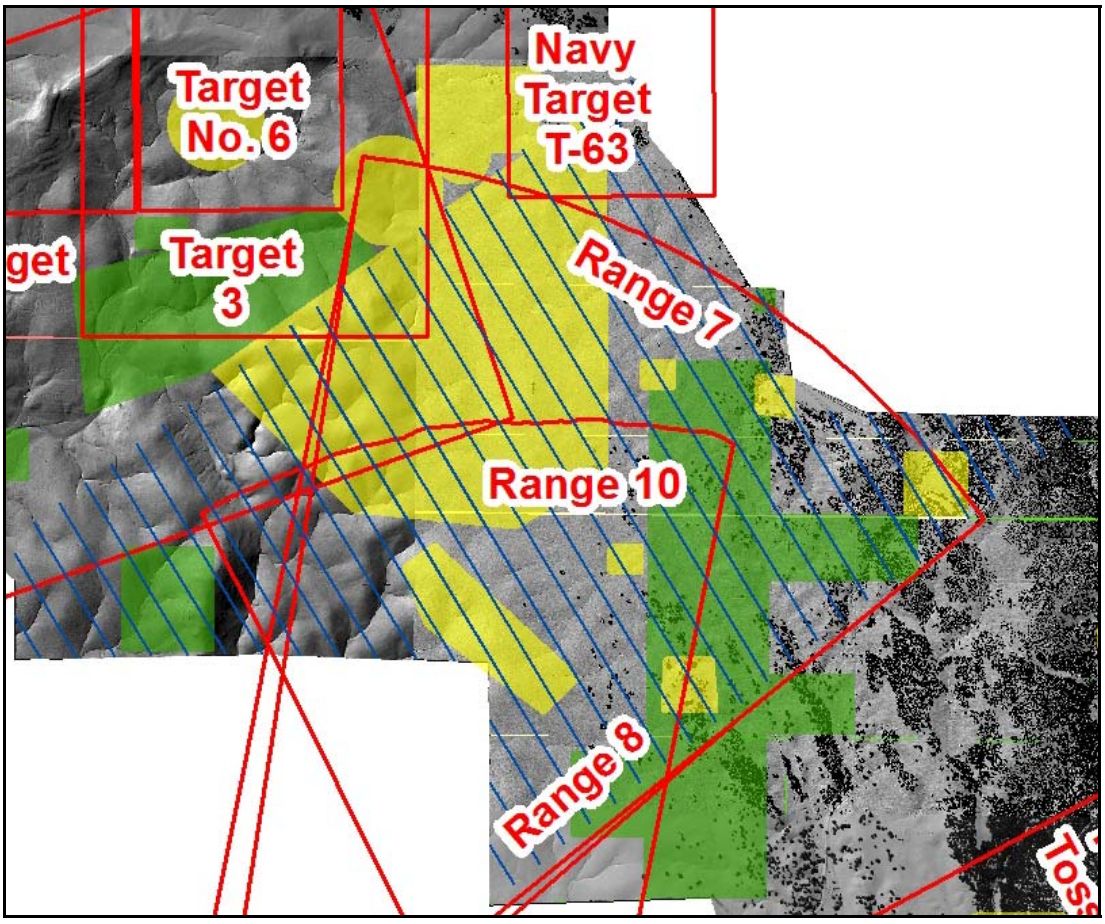

Figure 9. The 105-mm projectile transect design (blue lines) overlaid on a shaded relief of the lidar data for the central area of Camp Beale. The three ranges that lie almost entirely in this region are outlined in red and labeled. The yellow regions are those areas that show munition-related features based on the lidar data and the green regions show man made features that could be munitions related.

2.3. 81-mm Mortar Region

There are multiple ranges that lie within the 81-mm mortar region (i.e., the green portion of Figure 4). There is very little information about these ranges (shown by red outlines with labels in Figure 10), and the information generally does not include specific information about the smaller 37-mm and 81-mm mortars. The yellow and green shaded regions in Figure 10 identify the regions where man-made features were identified in the orthophotography and topographic lidar data. Many of the features located within this region were directly related to mortar practice ranges.

From a preliminary site meeting, the use of a 400-ft radius for the target area based on 37-mm munitions was proposed based on expert opinion regarding characteristic fragment throw distances. The PNNL/SNL team then verified that the fragment throw

distances estimated from the TP-16 report coincided with the decision made during the site meeting. The 400-ft radius target area did, in fact, fall between the conservative HFD of 200 ft and the MFD of 950 ft for 37-mm munitions.

However, based on further review of the orthophotography and topographic lidar data, ESTCP recommended that the smallest munition of interest within this region was an 81-mm mortar. From TP-16, the 81-mm M43 has an HFD of 230 ft and an MFD of 1395 ft. Because the estimates of the fragment throw distances for the 81-mm and the 37-mm munitions are similar, the assumed 400-ft characteristic target area radius established at the preliminary meeting was used in the green (southern) area of Figure 4 (81-mm mortar region).

The target detection performance curves shown in Figure 11 present the probability of traversing and detecting a 400-ft radius target area as a function of the transect spacing. The three colored lines show the sensitivity of the detection probabilities based on an average target area density of 40, 80, and 160 ApA above a background density of 45 ApA. The input values for the performance curves in Figure 11 are shown in Table 4.

The final transect spacing of 450 ft shown in Figure 11 has an approximately 92 percent chance of traversing and detecting any 400-ft radius target area having a bivariate normal distribution with an average density of 80 ApA above the background density of 45 ApA. This assumes that 1-m wide transects are gathered, the false negative rate is zero, and the flagged windows have at least a 95 percent confidence of being greater than background.

Table 4. The required traversal and detection inputs for the VSP calculations and the respective values used for this design.

VSP Inputs	Design Value
Transect Width	1 m
Transect Pattern	Parallel
Length of Semi-Major Axis	400 ft
Shape	Circular
Background Density	45 ApA
Decision Rule	95 percent
Instrument False Negative Rate	0
Target Area Density Above Background	40/80/160 ApA
Density Distribution	Bivariate Normal Density
Average Target Area Density Input as	Target Average
Minimum Precision/Maximum Error	0.1/0.05

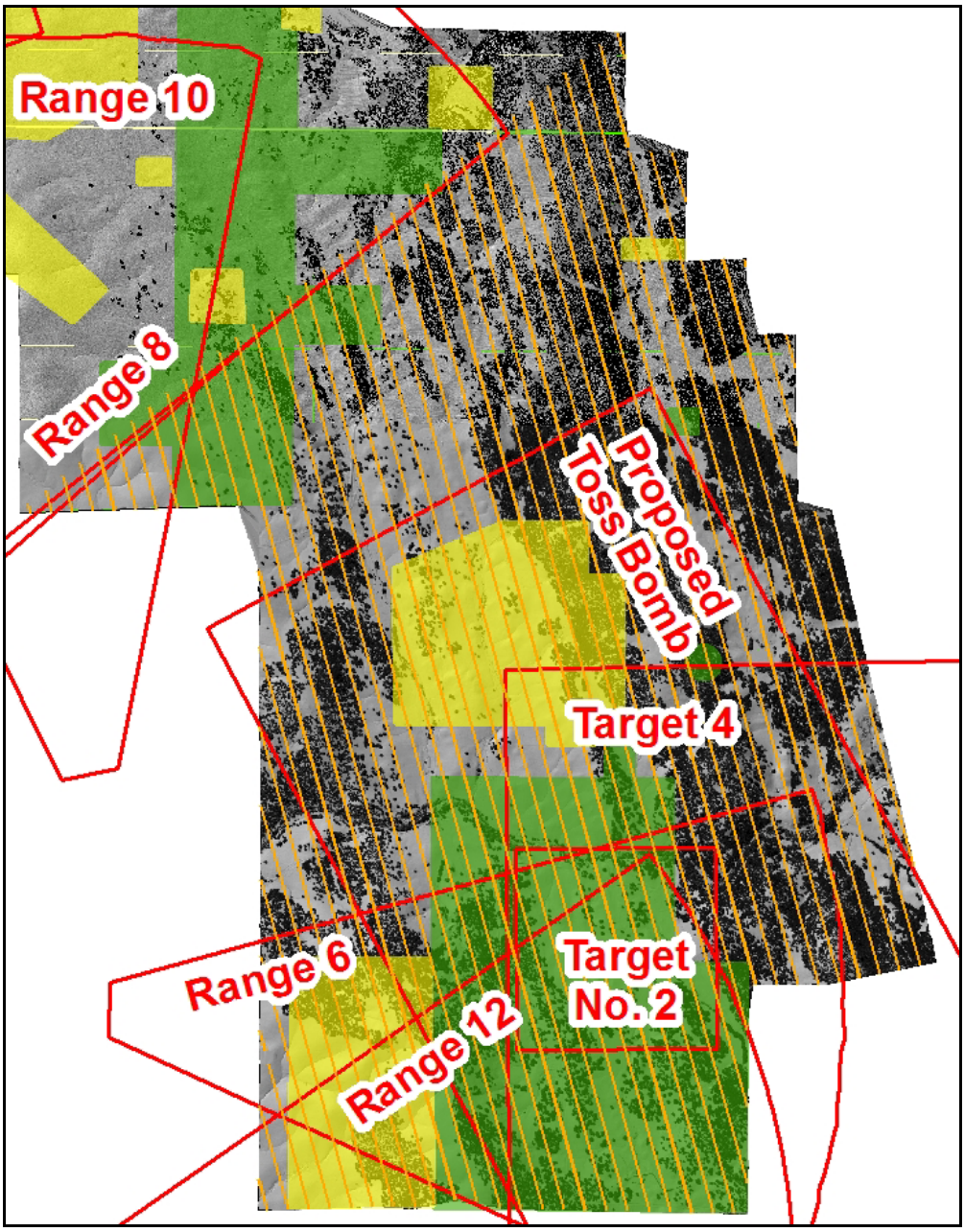

Figure 10. The 81-mm mortar transect design (orange lines) overlaid on a shaded relief of the lidar data for the southern part of Camp Beale. The historical ranges are outlined in red and labeled. The yellow and green regions are areas that show munition-related features based on the lidar data.

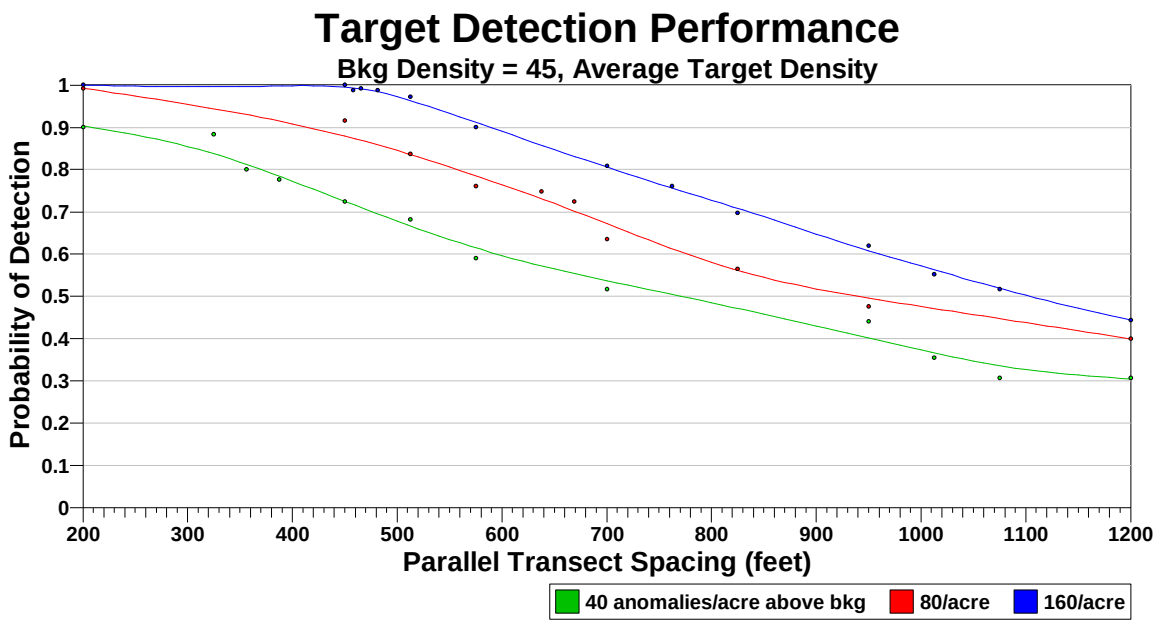

Figure 11. Power curves for the 400-ft radius target area based on the 81-mm mortars as a function of transect spacing. Each colored line represents a different density of the target area as labeled. The transect spacing of 450 ft was selected based on this graph.

2.4. Combined Site Transect Design Summary

There were three different transect designs for this site; a combined transect design summary is listed in Table 5 and shown in Figure 12. In summary, for the 100-lb bomb area (pink region in Figure 12), a 700-ft target area radius was assumed resulting in a transect spacing of 880 ft. The assumed target area radius and transect spacing for the 105-mm projectile area were 600 ft and 700 ft, respectively (yellow area in Figure 12); for the 81-mm mortar area (green area in Figure 12), a 400-ft target area was assumed resulting in a transect spacing of 450 ft. The geophysical survey team used two different sensor systems. One unit had a 1-m-wide footprint and the other had a 2-m-wide footprint. While some of the area within the 81-mm and 105-mm areas would be covered by both systems, the power curves shown in Figure 8 and Figure 11 are conservatively based on 1-m-wide transect coverage. Because of the open terrain at the north end of the site in the 100-lb bomb region, it was anticipated that the transects there would primarily be collected using the 2-m-wide transect system. Thus, Figure 6 is based on 2-m-wide transects. Tables 2 through 4 summarize the inputs for the three transect designs based on each of the munition-specific regions within the site. Table 5 summarizes the transect designs for the entire site as a whole.

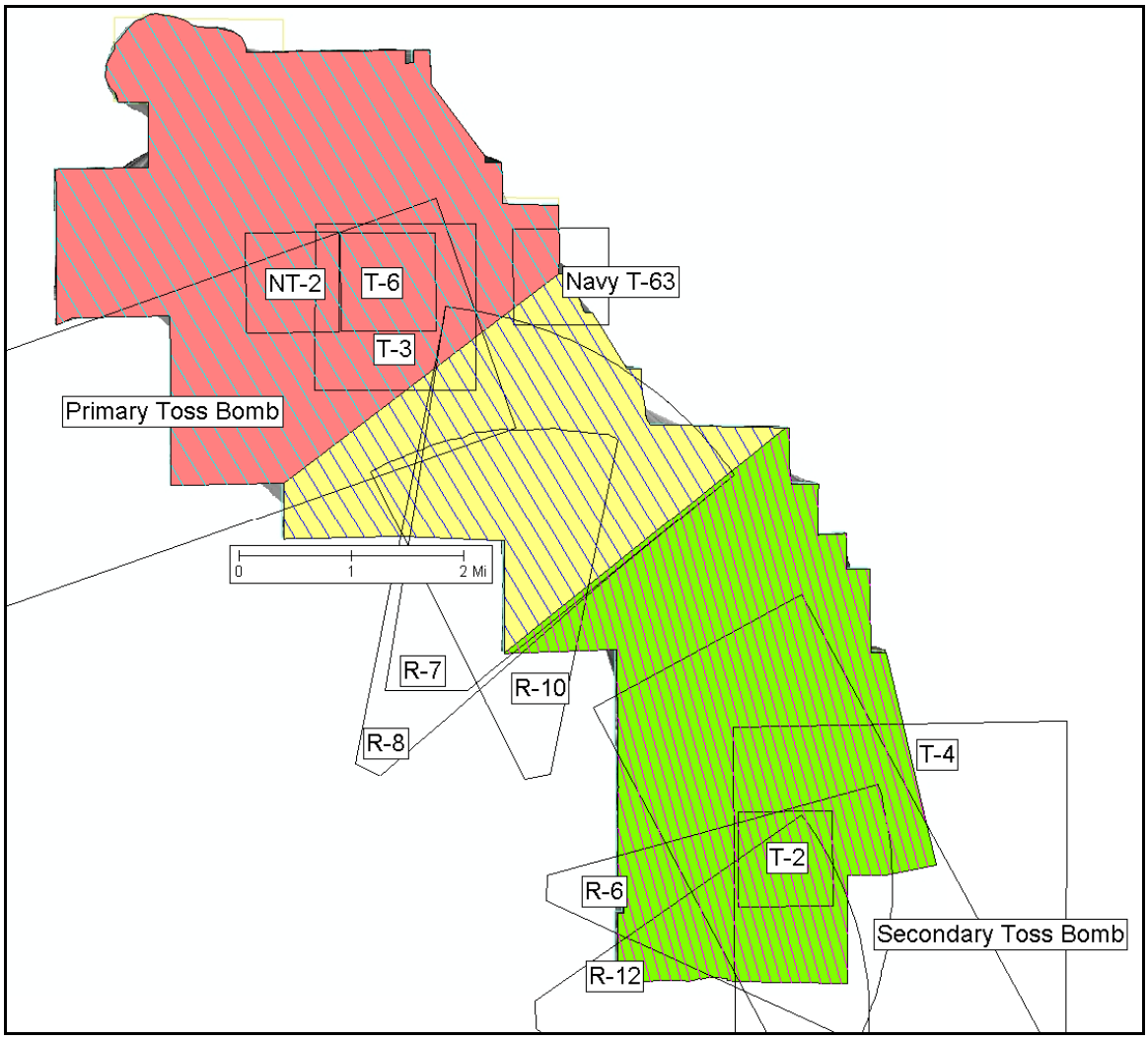

Figure 12. The entire Camp Beale WAA demonstration site showing each of the three finalized transect designs.

Table 5. Camp Beale site summary of the combined transect designs for the three munition-specific designs.

SUMMARY OF SAMPLING DESIGN	
Primary Objective of Design	Detect the presence of a target area that has a specified size and shape
Type of Sampling Design	Transect
Selected Sample Area	All
Area of Sample Area	18,261 ac
Shape of Target Area of Concern	Circular
Radii of Target Areas Of Concern	400,600, and 700 ft
Transect Pattern	Parallel
Transect Width	1 and 2 m
Computed Spacing Between Transect Centers	450, 700, and 880 ft
Probability of Traversing and Detecting the Target Area	> 90 percent
Probability of Traversing the Target Area	100 percent for all three target areas
Percent of Site Traversed	0.68 percent
Total Length of Transects	386 km

3. Analysis of Transect Survey Results

The analysis of the surveyed data based on the previously described transect designs is presented in the following sections. This analysis is based on the procedures described in Hathaway et al. (2008). The following sections use the flagging routines and geostatistical routines in VSP, described in section 3.1, to identify the high density areas within the Camp Beale WAA study area. Section 3.2 describes the reasoning for combining the 105-mm projectile and 100-1b bomb regions for the analysis stage. Section 3.3 examines the appropriateness of combining 1-m and 2-m transects for analysis; section 3.4 details the reasoning behind the selected window diameter for the analyses; section 3.5 provides the final flagged regions based on the selected window diameter and critical densities; section 3.6 uses geostatistical kriging routines to map anomaly density over the entire site; and section 3.7 provides the final delineations.

3.1. Window Density Calculation Algorithm

To identify the density of areas along transects, VSP passes a window over segments of the site and calculates the anomaly density for each segment. The window diameter specifies the size of the circular area over which the average density is computed. Figure 13 provides an example of how the window diameter is used to calculate transect grid densities. The window diameter defines the size of a centered circular window (orange and blue circles in Figure 13), which moves one-sixth of the selected diameter and uses the anomaly count with the transect area within the window to calculate a density assigned to the central transect grid (orange and blue boxes in Figure 13) centered in the

window. The green dots represent the identified anomalies within the two surveyed transects. This figure provides an example of two of the multiple transect grid densities that would be calculated based on these transects. These transect grid densities are used to calculate the ApA densities used throughout this report.

The selection of an appropriate window diameter is dependent on the size of the target area of interest, transect width, and spacing between transects. The optimum window diameter is one that has sufficient traversed area within the window without including such a large area that potential high-density areas can be masked by the surrounding low-density areas in the window. The blue window in Figure 14 provides an example of a window that is too large. If the window diameter is too small (red window in Figure 14), the limited amount of traversed area within the window is not sufficient to make accurate transect grid density estimates, which results in excessive "fliers" or isolated flags in different regions of the site. Within these two extremes, there often are many different window diameters that would be appropriate. Generally, the window diameter should be less than the diameter of the target area of interest and no smaller than the spacing between the original transect design. For a more detailed description of the VSP 5.0 algorithms and UXO analysis tools, see Hathaway et al. (2008). The process of selecting an appropriate window diameter for the Camp Beale site is described in section 3.4

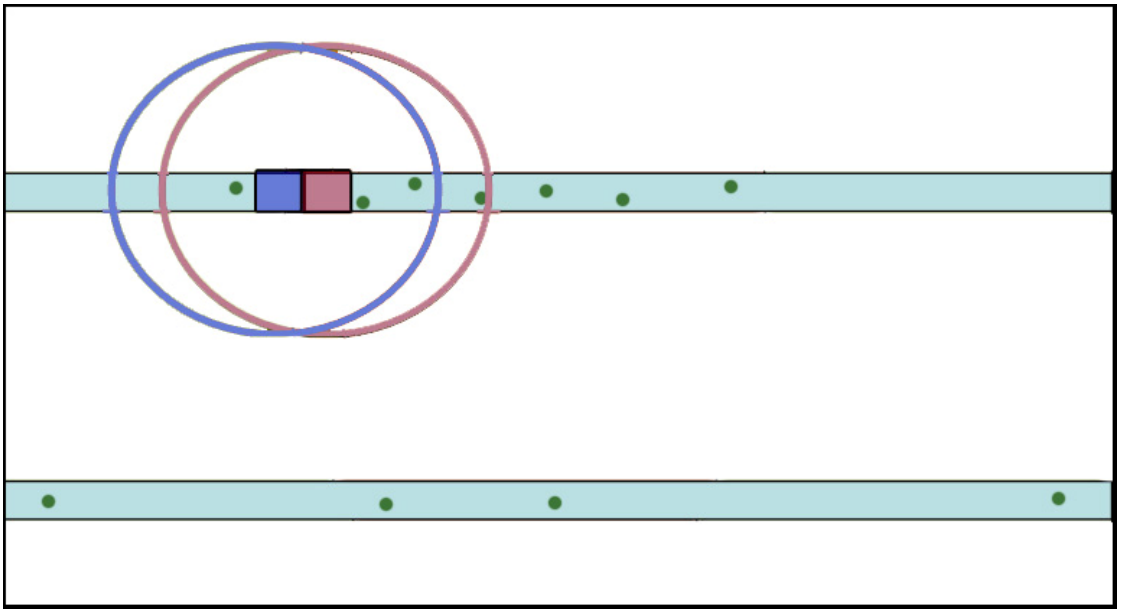

Figure 13. Depiction of the window-density calculation process used to identify high-density regions within a site.

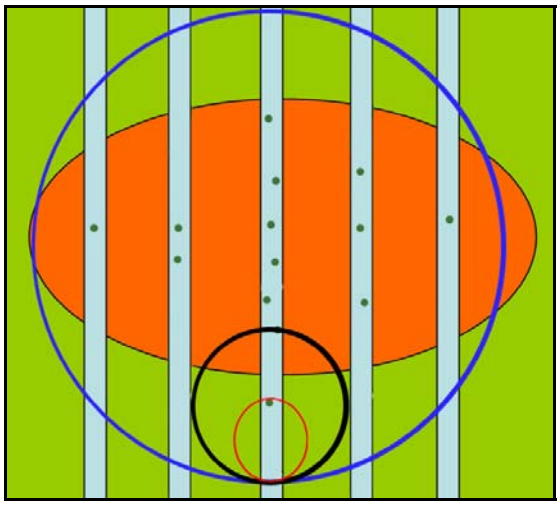

Figure 14. Example of different window sizes and how they would encompass the transect lines. The orange region is a schematic representation of a target area.

3.2. Preliminary Region Combination Analysis

While three separate regions were established for the transect design stage, the analysis procedures do not require that these regions be analyzed separately. If there is enough evidence to warrant the combination of regions, then a single analysis could be performed on the combined regions. Figure 15 shows some important features that aided in the final region combination decisions made for this site. The light blue boundary that overlaps the 105-mm and 100-lb bomb regions is a rough boundary of a large high magnetic anomaly density area. The manner in which this high-density area overlaps these two design regions suggests that they should be combined for analysis – section 3.5 provides more detail about this high-density area. In addition, the two northern areas were primarily surveyed using the 2-m towed array system (red lines), while the southern portion of the site was primarily surveyed using the 1-m manned portable system (green lines).

If the two areas have different background densities and require unique critical densities, then combining them for analysis would not be appropriate. The combination could potentially mask high-density areas in one region as a result of the higher critical density values in the other area. To examine this relationship between areas, the information from the data in the VSP-generated histograms shown in Figure 16 were used to create the plots shown in Figure 17. The histograms in Figure 16 were generated using a 400-m window based on the algorithm described in Section 3.1. For a more detailed description of how these density values are calculated, see Hathaway et al. (2008).

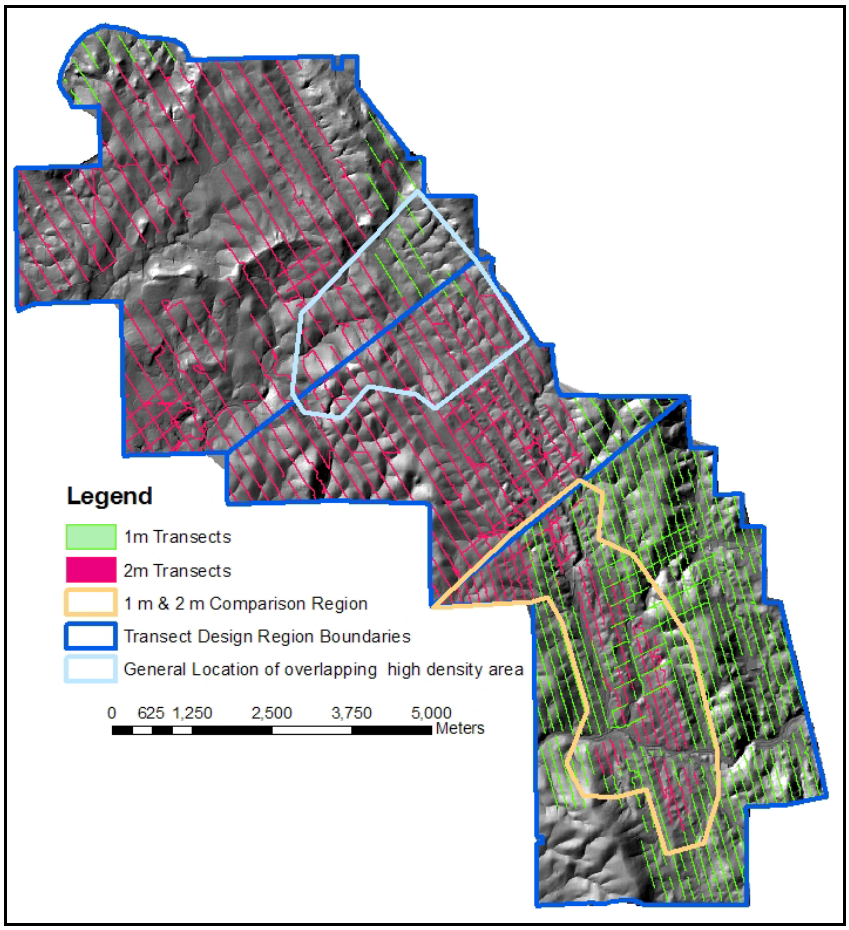

Figure 15. Surveyed 2-m (red) and 1-m (green) transects based on the previously described transect design.

Figure 17 provides a region-to-region comparison of the anomaly-density distributions among each of the regions. These plots, typically called quantile-quantile (QQ) plots, provide a graphical technique to determine if two different data sets are sampled from the same population. For Figure 17, the units are ApA, and the blue points represent the quantile values from the anomaly density samples in each region. The points should fall close to the diagonal black line if both regions have the same distribution of anomaly densities (i.e., the histograms shown in Figure 16 would have the same shape and spread). For evidence to combine or separate the regions, differences in the distributions for higher-density values are not as important as difference in the lower-density values. This results because the final critical density to flag high-density areas is selected within the lower-density values (0 to 200 ApA) and a large difference within this portion of the distribution could necessitate separate critical densities for each region.

From the three comparison plots, it appears that the 81-mm mortar and 100-lb bomb regions (lower plot) should not be combined as the difference from the grey line is large for anomaly density values between the 0 to 200 ApA range. However, the 105-mm projectile region does not appear to have as much difference from the other two regions

(top two plots). While the 105-mm projectile region could be combined with either of the other regions, from the plots in Figure 17, it is not clear if the 105-mm projectile region should be combined with the 81-mm mortar or 100-lb bomb region. However, based on the distribution of the 1-m and 2-m transects and the occurrence of an overlapping high-density area (Figure 15), the combination of the 100-lb bomb and 105-mm projectile regions is warranted. For all subsequent analyses the 100-lb bomb and 105-mm regions will be combined, and the 81-mm mortar region will be analyzed separately.

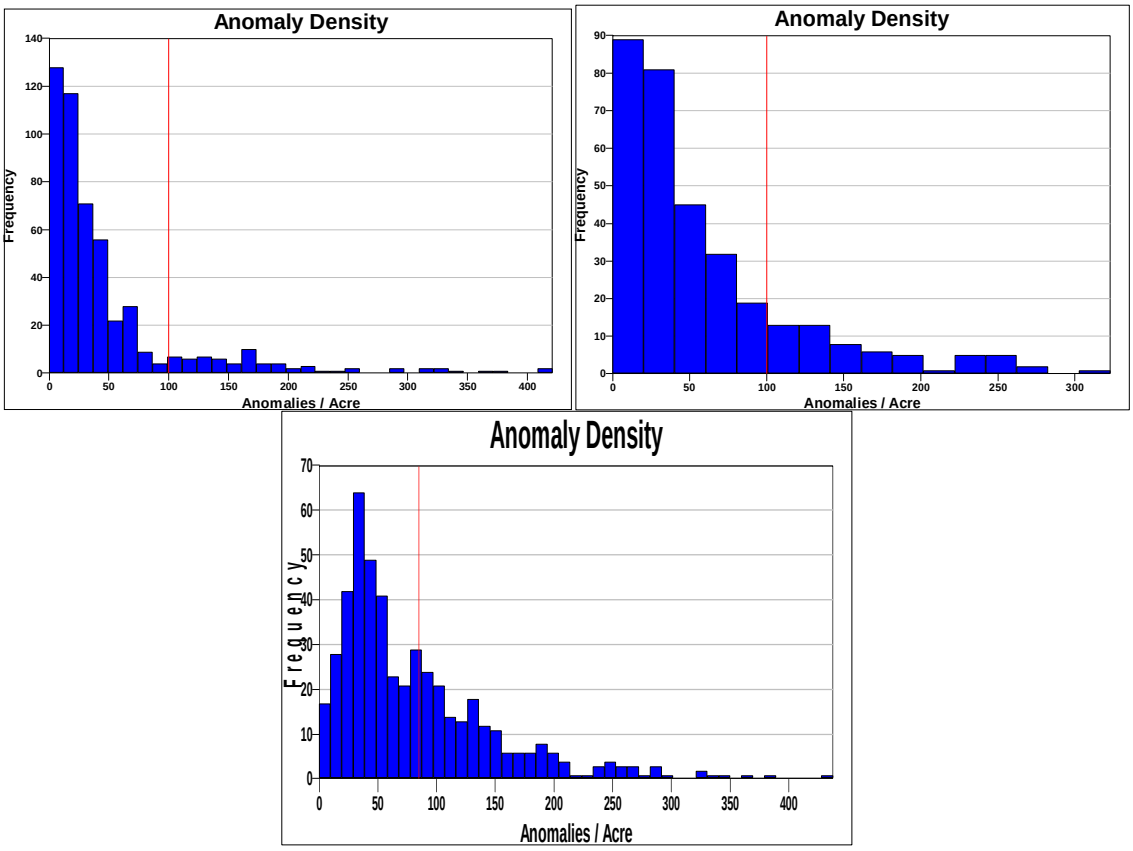

Figure 16. Histogram of the calculated transect grid densities using a 400-m window diameter for the 100-lb bomb region (top left), 105-mm projectile region (top right), and 81-mm mortar region (bottom).

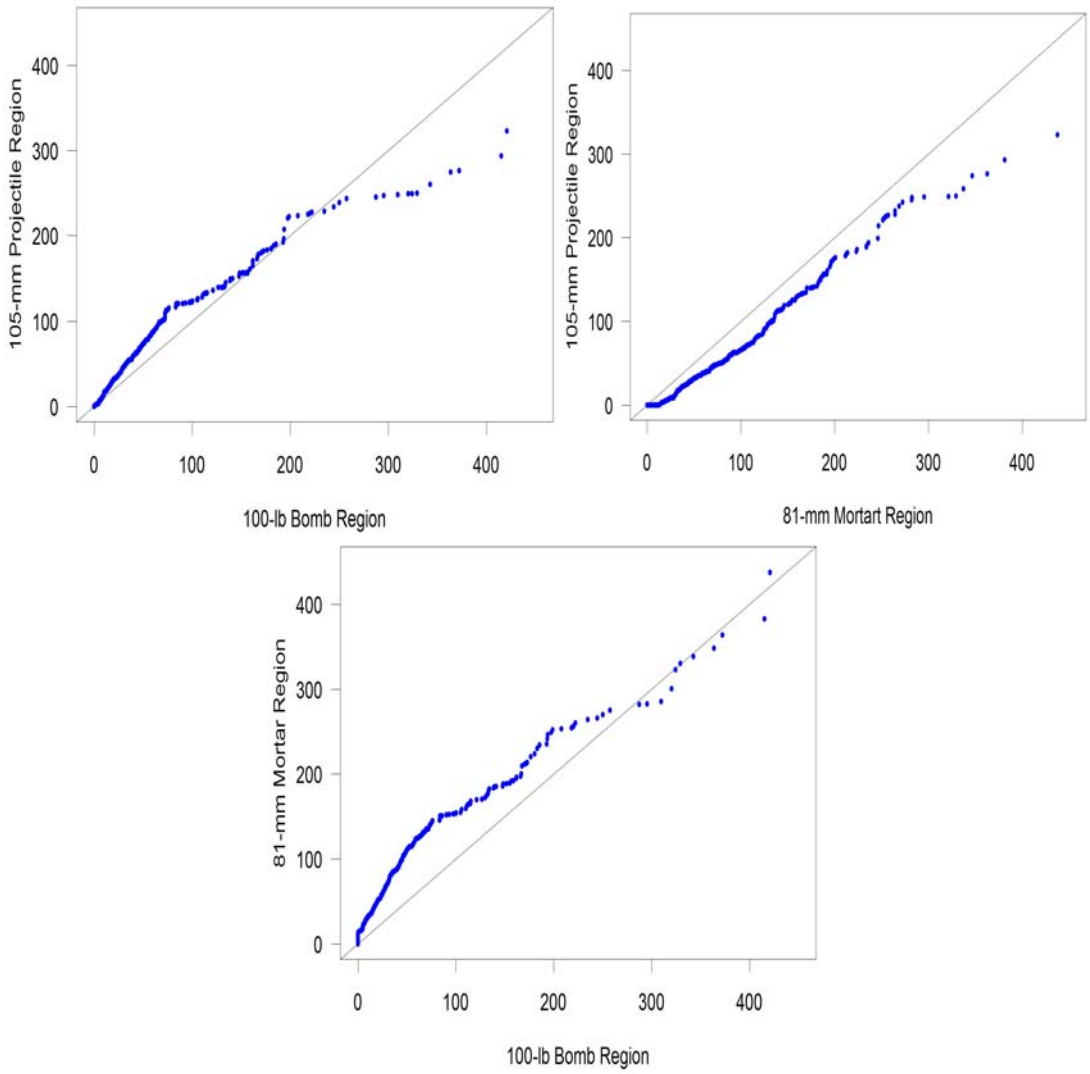

Figure 17. ApA comparisons among the three regions using a 400-m window diameter.

3.3. Combined Analysis of 1-m and 2-m Transects

It is feasible that the sensitivities and therefore anomaly density distributions could be different for the 1-m surveys than the 2-m surveys. If significant differences occurred, particularly between background density estimates, separate flagging and geostatistical analyses would be prudent on the results from each survey technology.

There are relatively few 1-m transects in the 100-lb bomb and 105-mm projectile regions, which limits the feasibility of analyzing each transect width separately. However, the 81-mm mortar region has a large area where both 1-m and 2-m transects were surveyed. This region is identified by a yellow boundary in Figure 15. The boundary of this region was defined to include all of the 2-m transects in this region and the 1-m transects that were reasonably close to the 2-m transects. Identifying surveyed transects from approximately the same region of the site reduced the effects of confounding the differences in effects between the survey systems and the differences in densities over the

site. Figure 18 provides a QQ plot that compares the distribution of anomaly densities within the overlapping region between the 1-m transects and the 2-m surveyed transects. While there is some variation, it appears that the densities from the 1-m and 2-m transects follow the same density distribution and can be combined for analysis.

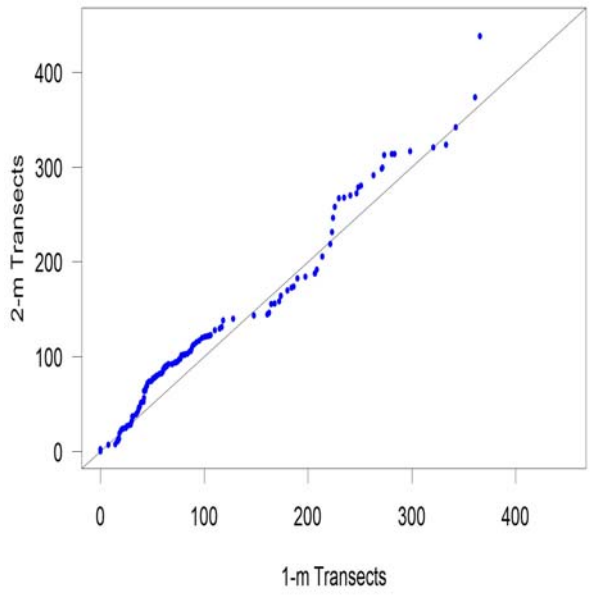

Figure 18. Comparison of ApA densities for the 1-m and 2-m transects surveyed in a subset of the 81-mm mortar region.

3.4. Camp Beale Window Size Selection

While it is difficult to convey the entire procedure of selecting an appropriate window diameter, this section attempts to show some of the different window diameters that were examined for the Camp Beale study. Figures 19 and 21 show some of the results from the process of selecting an appropriate window diameter.

Figure 19 displays the multiple-flagged region overlays using varied window diameters based on a 100 ApA critical density, and Figure 20 shows the flags for each one the window diameters separately. These flagged regions show areas with anomaly densities at or above the critical density. The 1200-m and 800-m diameter windows (green and purple) are the largest windows used, and the boundaries are displayed in Figure 19. Figure 20 shows the flags for both of these window diameters. The 400-m and 300-m window diameter flags are overlaid in Figure 19, and are shown separately in Figure 20. All of the displayed window diameters generally identify the same high-density regions on the site. The primary differences between the results from the window sizes are on the perimeter of the larger high-density regions and in the identification and location of the smaller flagged regions. This is a result of the selected window diameter; however, some of the difference in flagging can also be attributed to using a 100-ApA critical density for each window diameter. As the window size gets larger, there are changes in the

distribution of densities, and it is possible that each window would require a unique critical density to be acceptable.

Figure 21 provides an example of the anomaly density distribution for the 81-mm mortar region when different window diameters are selected. For display purposes, box-plots are used to display the distribution of anomaly densities associated with each window diameter. The box-plots show that the results from the smaller window diameters tend to be skewed to the higher densities and have more zero-density values. However, the interquartile range (values observed between 25 percent and 75 percent) are reasonably similar. The largest differences are between the 300-m and 1200-m window diameters.

Comparing the flagged regions from 300-m window diameter (light blue) to the 1200-m diameter window (green) flagged regions in Figure 19 provides an example of the concepts described in Section 3.1. The 300-m window diameter creates the most fragmented flagging because the averaging window is too small. The 1200-m window has very few isolated flags, but it does not flag some smaller regions that the other three window diameters identify as high-density areas because they are averaged in with background densities. The 400-m window diameter is used throughout this report for any analysis and comparisons as it maintains the detail without causing many isolated and possibly erroneous flags.

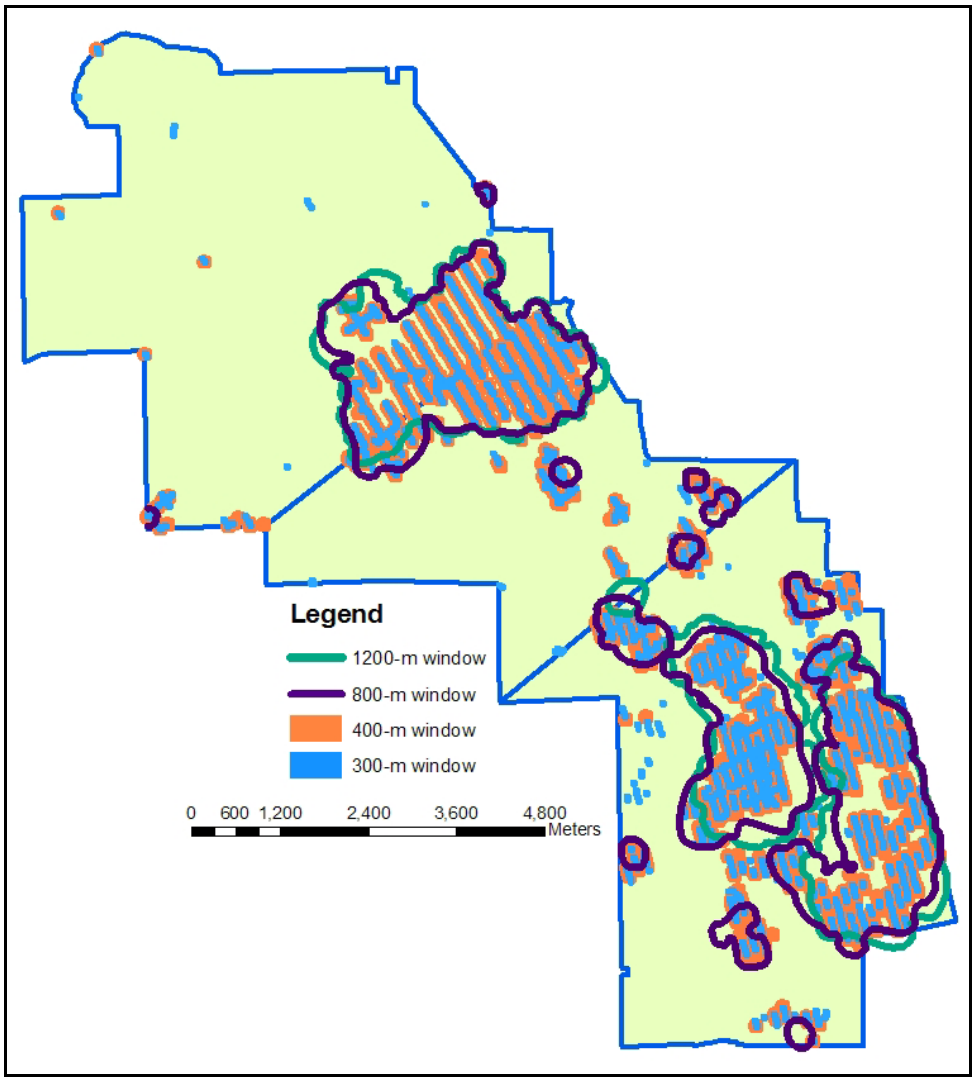

Figure 19. Flagged region overlays based on a 100-ApA critical density using multiple window diameters, as labeled. Two larger window diameters are represented by an outline of the flagged regions.

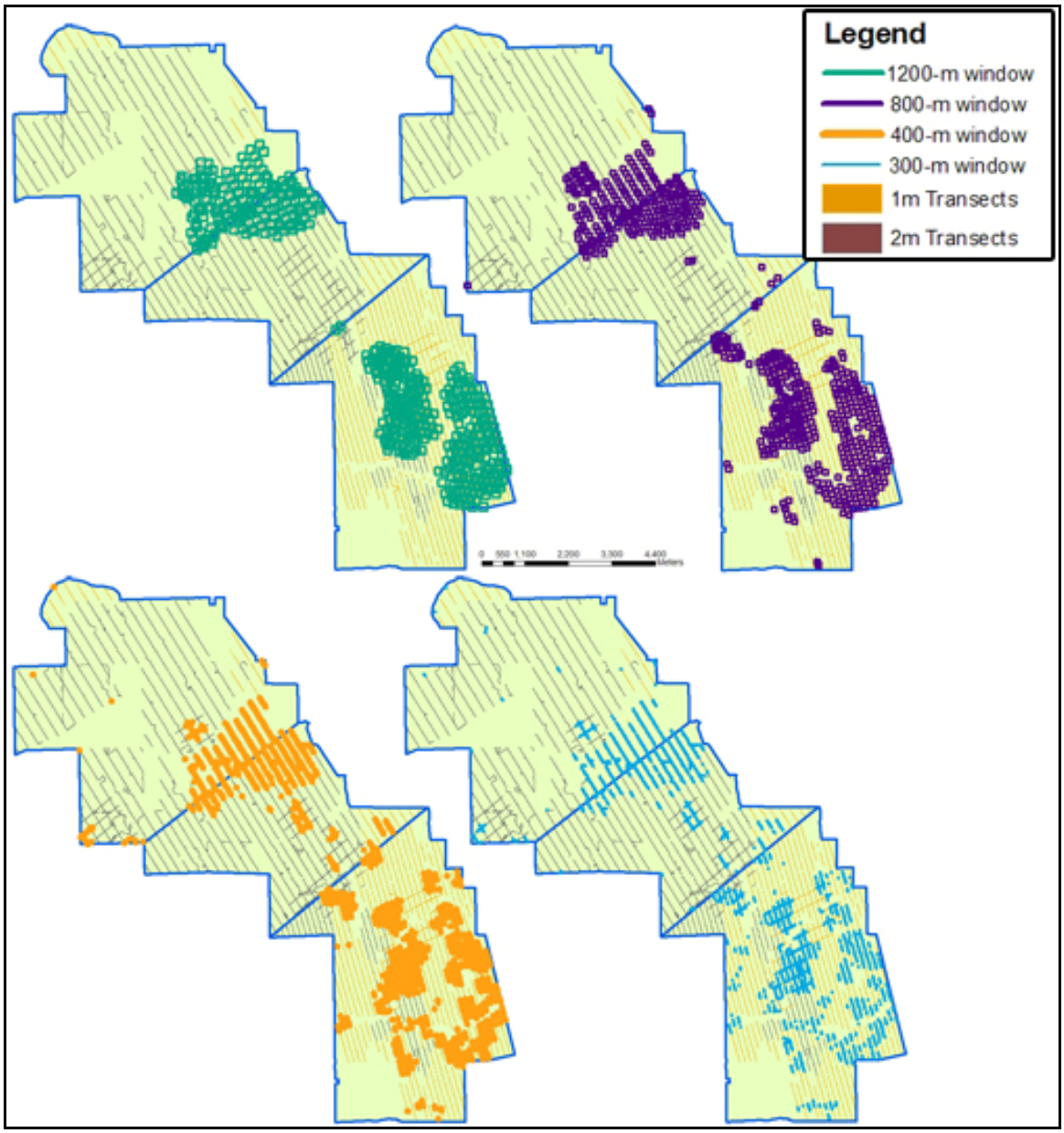

Figure 20. Separate maps of the flagged regions using the four window diameters, as labeled, with a 100-ApA critical density.

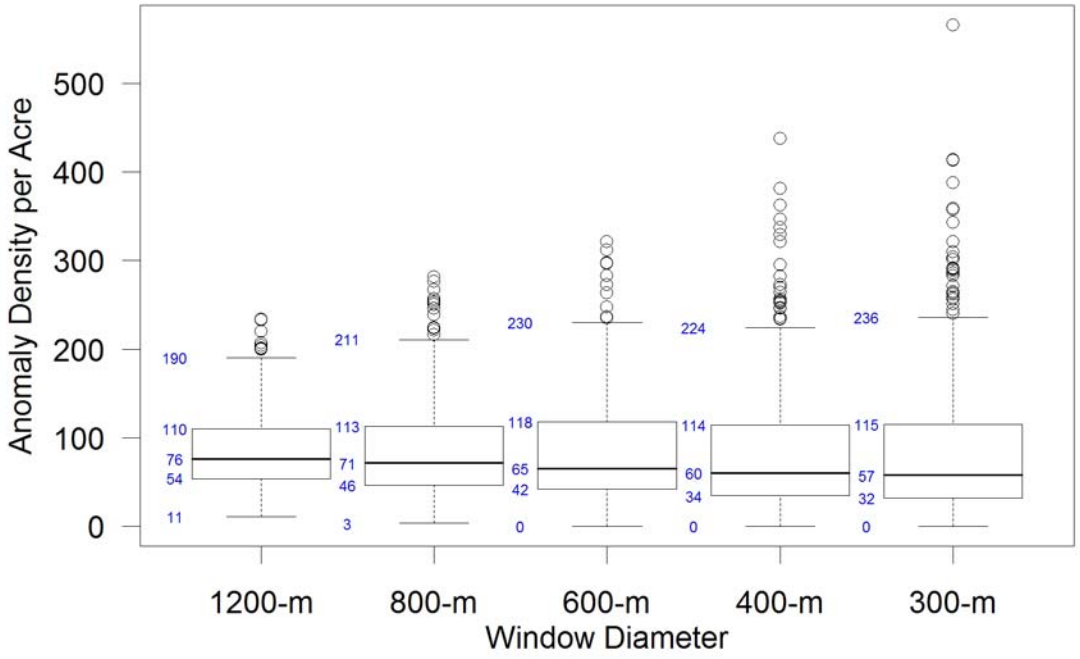

Figure 21. Box-plots of the densities from the southern 81-mm region based on different window diameters as labeled.

3.5. Transect Density Histograms and Flagging Analysis

The final critical density for the combined 100-lb bomb and 105-mm projectile regions was selected using Figure 22 while examining the flagged areas resulting from different critical densities. The final critical density of 95 ApA (red line in Figure 22) produced the flagging results shown in Figure 23. This critical density was difficult to determine from the histogram alone. Looking at the location of flags throughout the region for different critical densities aided in the selection of 95 ApA as the critical density value. This critical density minimized the number of isolated flags while maintaining the flags in the regions with multiple flags.

Figure 24 and Figure 25 show the histogram of window densities and the resulting flagged regions for the 81-mm mortar region, respectively. The histogram in Figure 24 appears to have an inflection point between 75 ApA and 100 ApA. The final selected critical density of 85 ApA (red line in Figure 24) falls within these values and marks the flagged regions shown in Figure 25. This region has the largest percentage of flagged areas as compared to any of the other analyses performed as a part of the WAA demonstration. The large percentage of the site having flagged areas makes it more difficult to optimize the critical density by minimizing the number of isolated flagged regions. But, as with the northern portion of the site, the final critical density minimized the number of isolated flags while maintaining the regions with multiple flags.

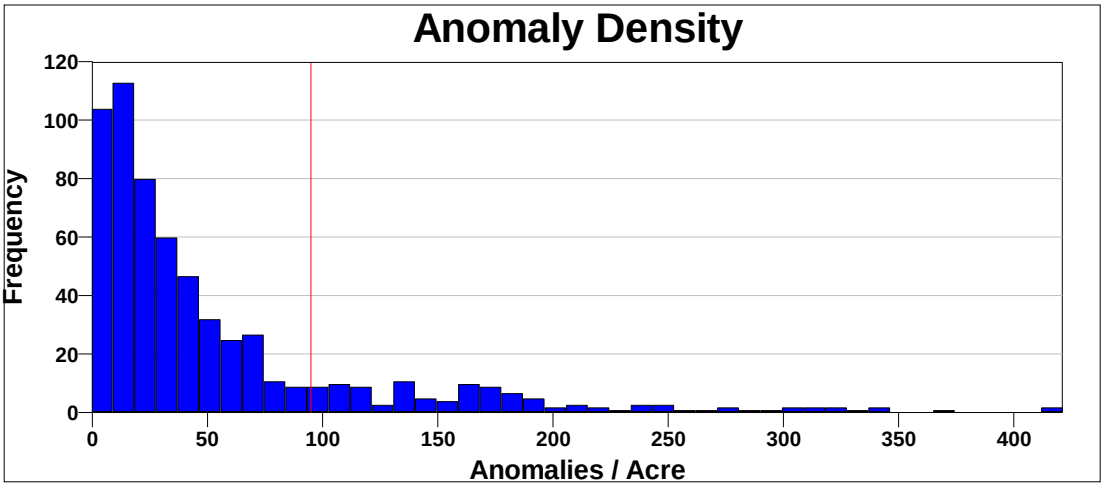

Figure 22. Histogram of window densities in ApA for the combined 100-lb bomb and 105-mm projectile regions. The red line marks the critical density of 95 ApA.

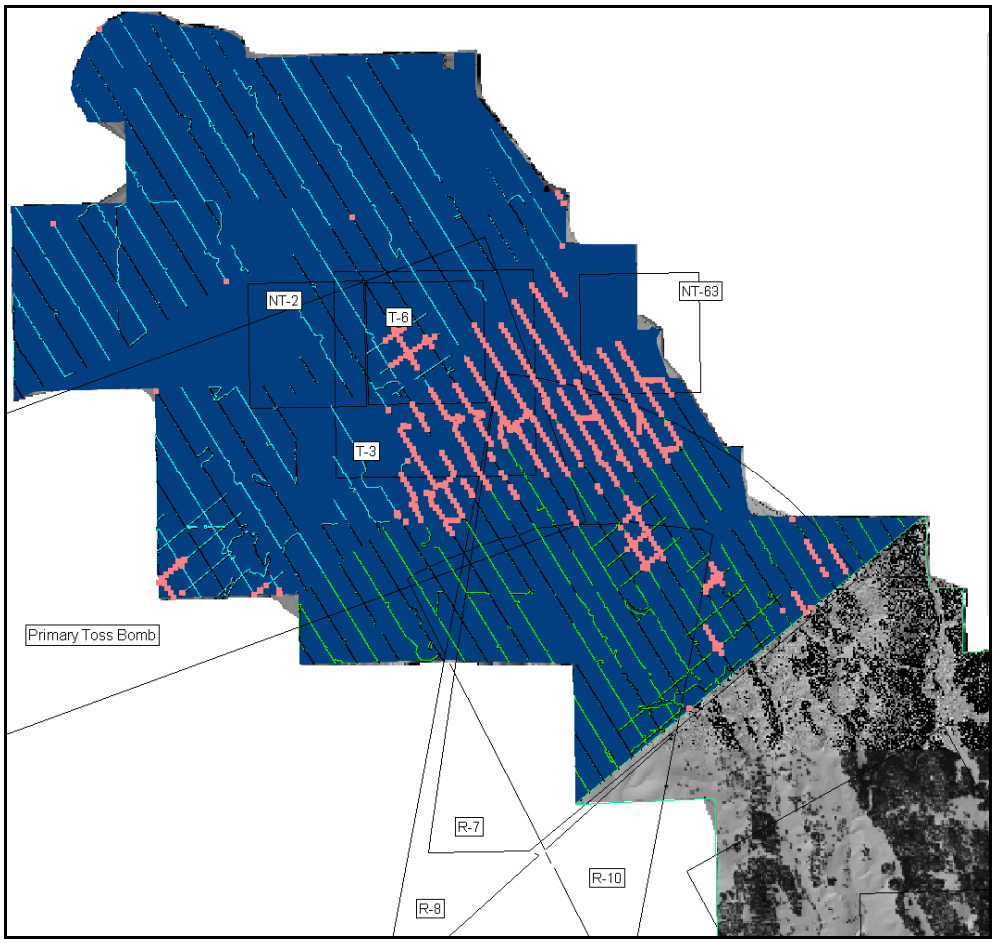

Figure 23. Flagged regions in the combined 100-lb bomb and 105-mm projectile regions based on a 95-ApA critical density.

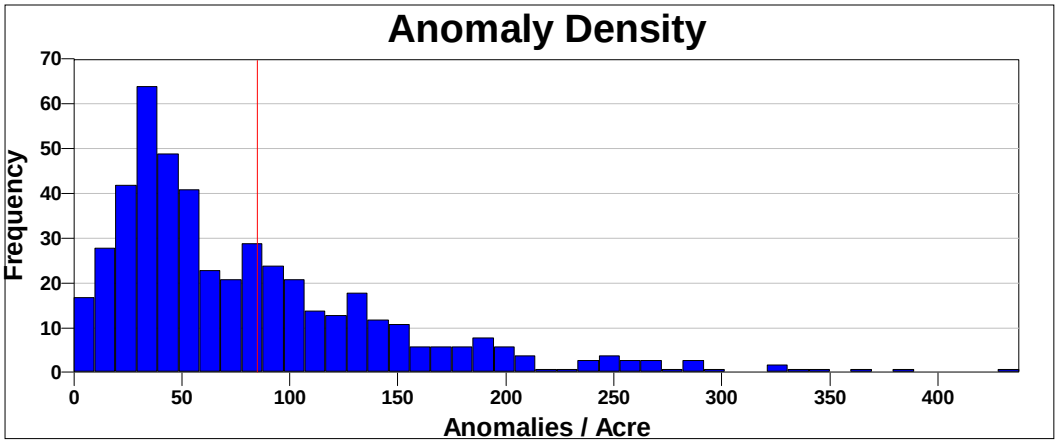

Figure 24. Histogram of window densities in ApA for the 81-mm mortar region. The red line marks the critical density of 85 ApA.

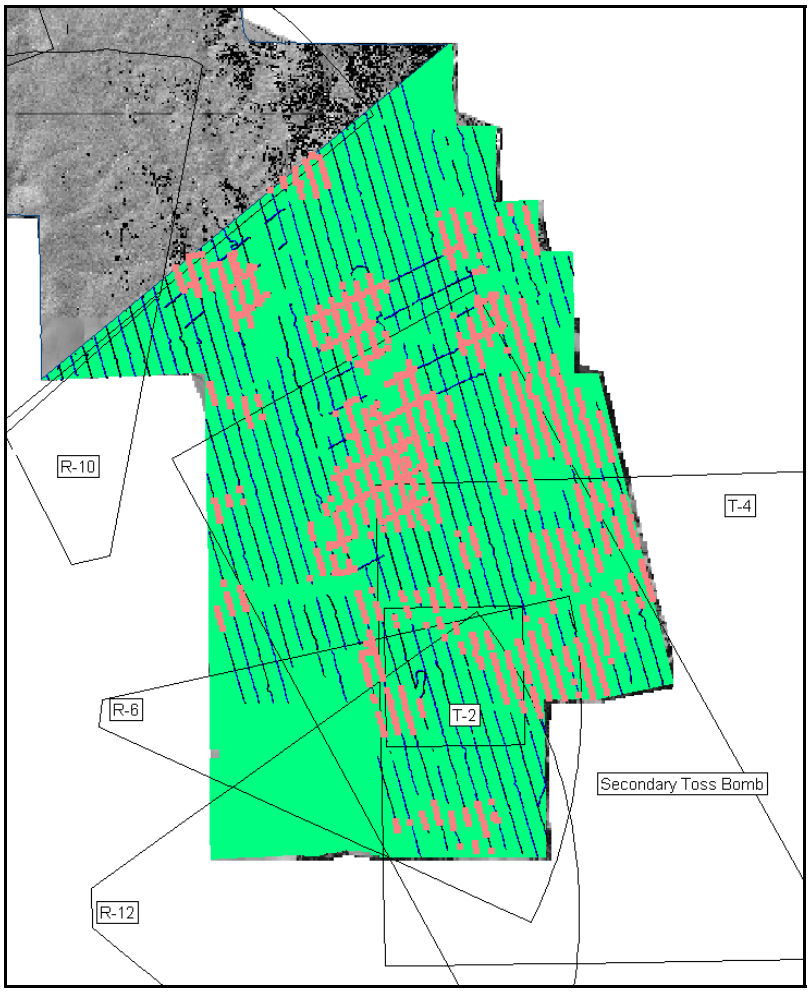

Figure 25. Flagged regions in the 81-mm mortar region based on an 85-ApA critical density.

3.6. Geostatistical Density Mapping

To assist in the delineation of areas with high anomaly densities, geostatistical (kriging) estimates of anomaly density were developed using the sample transect data. The geostatistical estimates provide values of anomaly density at unsampled areas away from the survey data transects and, therefore, provide a more comprehensive depiction of anomaly density patterns across the study area relative to flagging locations along the transects. This comprehensive depiction is valuable in the selection of high-density areas that may represent former target locations.

As with the other analyses presented in this report, the geostatistical analysis of the Camp Beale study area was conducted using two separate regions. The 100-lb bomb and 105-mm projectile areas were combined into a single analysis region that encompasses the northwestern two-thirds of the WAA study area. The remaining one-third of the site, which includes the 81-mm mortar area, was the second analysis region.

The geostatistical analyses were conducted within the VSP software package. The same magnetic anomaly location and course-over-ground data used in other VSP analyses presented in this report also were used directly in the geostatistical analyses. In addition, the same averaging window (400 m) used in previous sections of this report was adopted for all the geostatistical analyses.

3.6.1. 100-lb bomb/105-mm projectile area geostatistical analysis

As previously discussed, the 100-lb bomb and 105-mm projectile transect sample areas were combined into a single analysis region. All the transect and anomaly data from both of these sample areas, including all 1-m and 2-m transects, were combined and used as a single sample data set for the geostatistical analysis. The transect-based anomaly density values were computed from the anomaly location data and the transect survey area using a 400-m averaging window (section 3.4). It is these transect-based anomaly density data that were then used in the geostatistical analysis.

The initial step in the geostatistical analysis was the development of the variogram model. The spatial structure of the transect-based anomaly density data was investigated using an empirical variogram that depicts how the variability of the transect-based anomaly density data changes with increasing distances between the observational data. With most spatially dependent data sets, the typical situation is for the variability to increase with increasing distance between observations.

As shown in Figure 26, the empirical variogram from this data set follows the expectation of increasing variability with increasing separation distance. Figure 26 shows the empirical variogram values (black dots) and the functional model fit to those data (green line). The variogram model was manually fit to the empirical data using two separate functions. The final model represents the combination of these two functions. The parameters for these functions are discussed later in the text and are presented in Table 8.

The combined variogram model was then used directly by the kriging estimator in the development of the estimates of anomaly density.

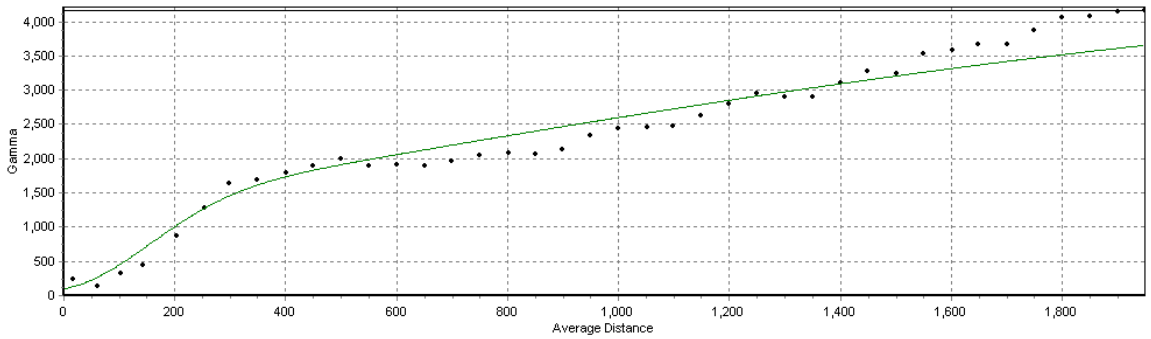

Figure 26. Variogram for 100-lb bomb and 105-mm projectile combined analysis area. The black dots represent empirical data; the green line represents the functional model fit to the empirical data.

The kriging estimator within the VSP software package generates estimates for a grid of points covering the area of interest. For the estimates considered here, a grid with an equal spacing of 50 m for both the X and Y directions was used. This grid was oriented so that the X direction and Y direction were parallel to the east-west and north-south geographic directions, respectively. The kriging estimates were conditioned to the available observational data (i.e., the estimates at unsampled locations were based on weighted averages of the surrounding observational data). A maximum search radius for the inclusion of observational data was set to increase computational efficiency and to maintain the effect of local variations in the observational data. A maximum search radius of 400 m was used in the kriging of the combined 100-lb bomb and 105-mm projectile analysis area. Although, the use of the 400-m search radius did maintain the integrity of local features, it did result in some limited areas where estimates could not be made because of insufficient data. If sufficient data were not available for the kriging estimator, that location was flagged as being "unestimated." This notation is desirable because it prevents the generation of estimates for regions that are far removed from any observational data.

Figure 27 shows the results from the kriging estimation of anomaly density for the combined 100-lb bomb and 105-mm projectile analysis area. In this figure, there are several higher-density (> 100 ApA) areas situated across the site. The largest of these areas is located near the center of the analysis area and appears to be composed of several subareas that may overlap. Note that the circular area where the anomaly density is the highest directly corresponds with one of the observed target circles. The general background anomaly density values appear relatively high, with a large percentage (> 80 percent) of the analysis area having density values above 10 ApA (Figure 28). Some regions of the analysis area are not color-shaded because no kriging estimate was generated there because no observational data were available.

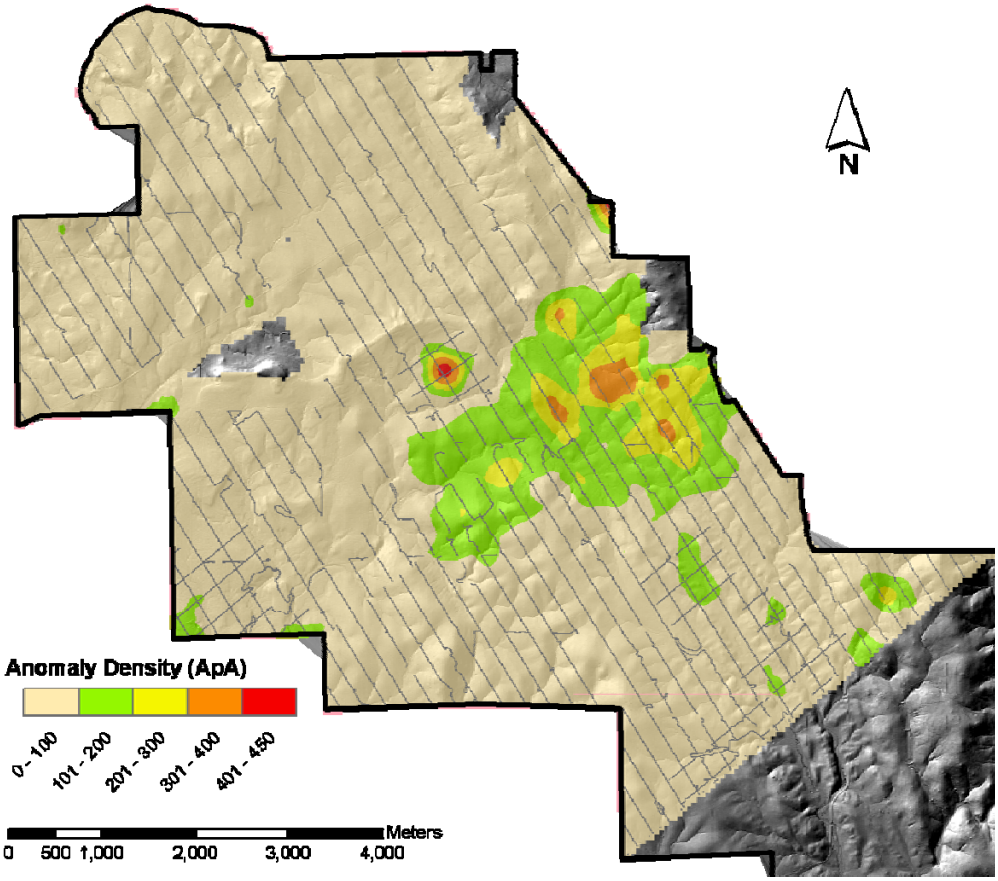

Figure 27. Anomaly density values (ApAs) for the 100-lb bomb and 105-mm projectile combined analysis area. Areas without color shading were not estimated because no observational data were available. Gray-colored lines show transect sample locations.

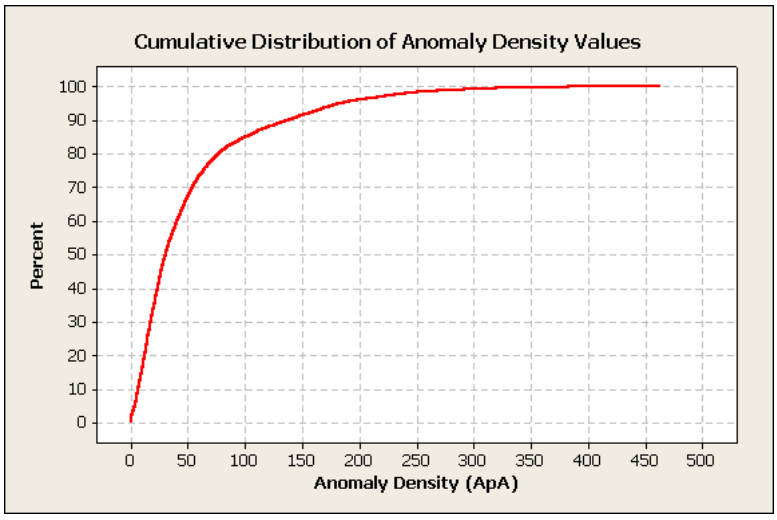

Figure 28. Cumulative distribution of estimated anomaly density values for the 100-lb bomb and 105-mm projectile combined analysis area.

Table 6 gives some basic information regarding the kriged estimate of anomaly density for the combined 100-lb bomb and 105-mm projectile analysis area.

Table 6. Basic statistics for the kriged estimates of anomaly density for the combined 100-lb bomb and 105-mm projectile analysis area. The minimum and maximum density values are estimated within a single 50 x 50-m grid cell.

Statistic	Value
Total Area (ac)	11,484
Total Anomaly Count (Estimated)	603,957
Minimum Anomaly Density (ApA)	0.0
1st Quartile (ApA)	14.7
Mean Anomaly Density (ApA)	52.6
3rd Quartile (ApA)	63.9
Maximum Anomaly Density (ApA)	463.0

3.6.2. 81-mm mortar area geostatistical analysis

As previously described, the 81-mm mortar transect sample area was handled as a separate analysis region independent from the other portions of the Camp Beale WAA site. All the transect and anomaly data from the 81-mm mortar sample area, including all 1-m and 2-m transects, were combined and used as a single sample data set for the geostatistical analysis. Similar to the other analysis area, the transect-based anomaly density values were computed from the anomaly location data and the transect survey area using a 400-m averaging window (section 3.4). It is these transect-based anomaly density data that were then used in the geostatistical analysis.

Similar to the previously presented geostatistical analysis, the initial step in the geostatistical analysis was the development of the variogram model. Figure 29 shows the empirical variogram values (black dots) and the functional model fit to those data (green/ red line). The variogram model was manually fit to the empirical data using two separate functions. The final model represents the combination of these two functions. The parameters for these functions are discussed later in the text and are presented in Table 9. The combined variogram model was then used directly by the kriging estimator to estimate the anomaly densities.

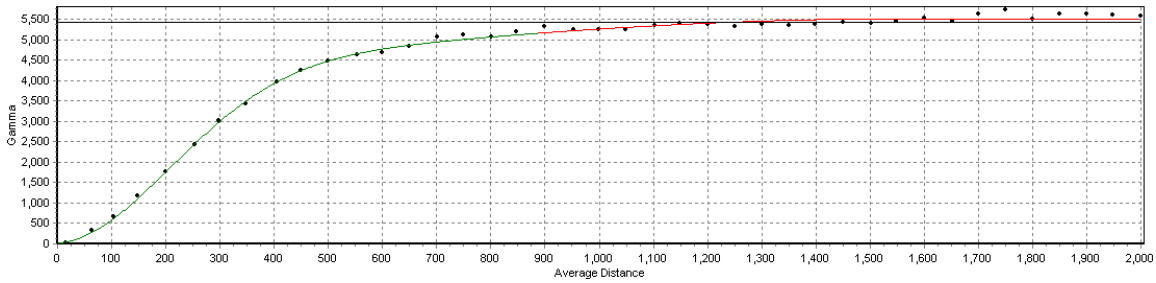

Figure 29. Variogram for the 81-mm mortar analysis area. Black dots represent empirical data; the line that transitions from green to red represents the functional model fit to the empirical data.

Similar to the previous kriging estimates, for the 81-mm mortar analysis area, a grid with 50-m spacing for both the X and Y directions oriented parallel to the cardinal directions was used. In addition, the same 400-m maximum search radius was used during the kriging process.

Figure 30 shows the results from the kriging estimation of anomaly density for the 81-mm mortar analysis area. In this figure, there are several higher-density (> 100 ApA) areas situated primarily within the eastern half of the site. In general, the higher-density areas are fairly dispersed; however, several isolated, very-high-density (> 300 ApA) areas are identifiable in the kriging results. Similar to the combined 100-lb bomb and 105-mm projectile analysis area, the general background anomaly density values appear relatively high, with a large percentage (> 90 percent) of the analysis area having density values above 10 ApA (Figure 31). Areas in the figure without color shading were not estimated because no observational data were available.

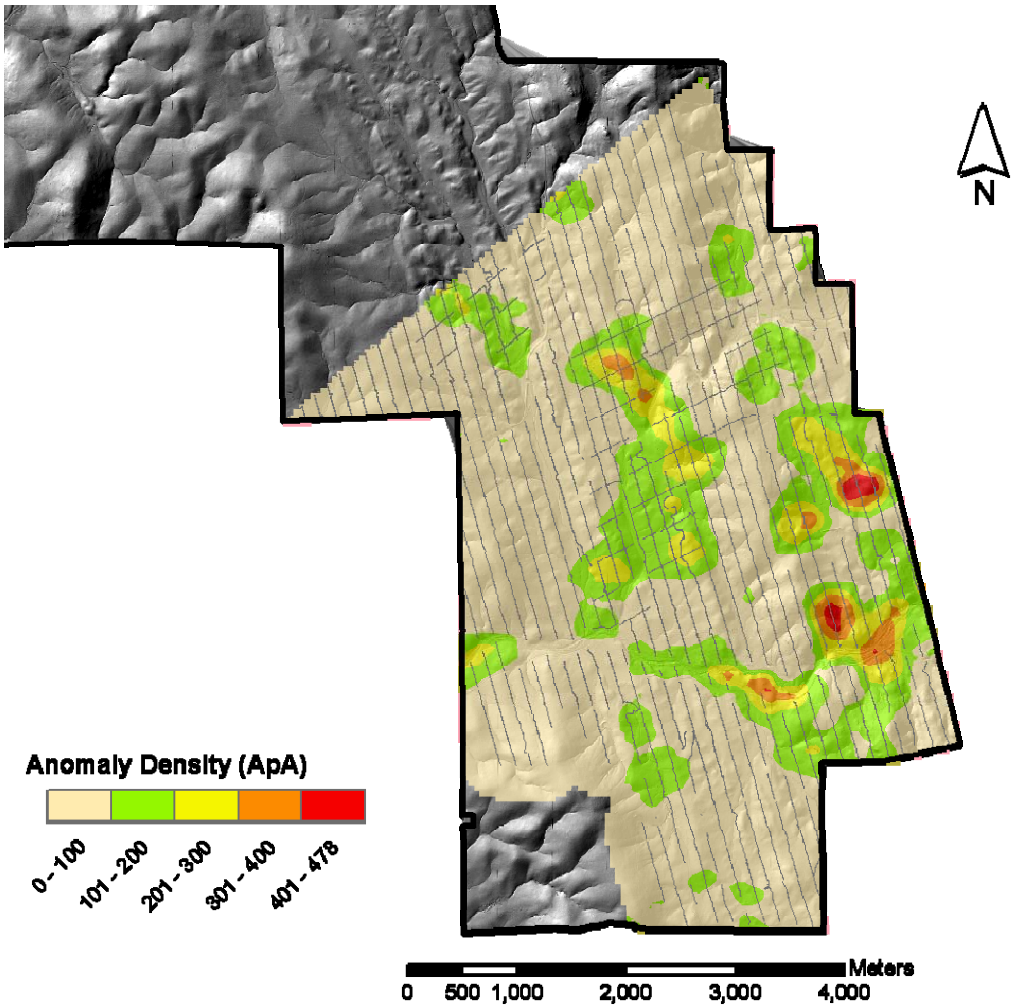

Figure 30. Anomaly density values (ApAs) for the 81-mm mortar analysis area. Areas without color shading were not estimated because no observational data were available. Gray lines show transect sample locations.

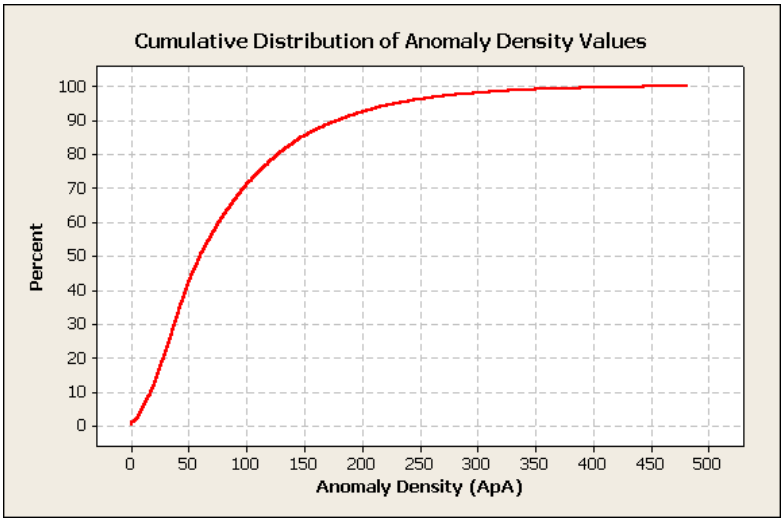

Figure 31. Cumulative distribution of estimated anomaly density values for the 81-mm mortar analysis area.

Table 7 gives basic information regarding the kriged estimate of anomaly density for the 81-mm mortar analysis area. Compared to the combined 100-lb bomb and 105-mm projectile analysis area, the kriging results from the 81-mm mortar analysis area have a higher overall anomaly density (Table 6, Table 7). This is based on the 1st and 3rd quartile values as well as the mean and maximum anomaly density values. In addition, the cumulative distribution curve for the 81-mm mortar analysis area has a much smoother curve in the transition from the low- to high-density values (Figure 31). Contrast this with the more abrupt break in slope and steeper initial climb of the cumulative distribution curve for the combined 100-lb bomb and 105-mm projectile analysis area (Figure 28).

Table 7. Basic statistics for the kriged estimates of anomaly density for the 81-mm mortar analysis area. The minimum and maximum density values are for a 50 x 50-m area.

Statistic	Value
Total Area (ac)	6,393
Total Anomaly Count	528,928
Minimum Anomaly Density (ApA)	0.0
1st Quartile (ApA)	33.2
Mean Anomaly Density (ApA)	82.7
3rd Quartile (ApA)	111.0
Maximum Anomaly Density (ApA)	482.0

3.6.3. Variogram sensitivity analysis

The initial step in developing geostatistical estimates of anomaly density is the modeling of the spatial structure of the observational data using a variogram. A basic sensitivity investigation to demonstrate the impact of the variogram modeling on the final kriging

results is discussed below. This sensitivity analysis provides only a brief example of the impact of changes in the variogram on the final results, but the example is pertinent in that it addresses the two major application modes of the UXO geostatistical analysis module within the VSP software package.

To investigate the impact of variogram sensitivity on the final results, two different variogram models were used to generate kriging estimates for the combined 100-lb and 105-mm projectile analysis area. These two variogram models were the manually-fit model used in the geostatistical analysis discussed above and the automatically-fit model that is generated by the VSP UXO module when the geostatistical analysis is run in the automatic mode. All other parameters involved in the kriging analysis were held constant; the only variable that changed between the two analyses was the variogram model used in the kriging.

Figure 32 shows the variogram models used in the analysis for the combined 100-lb bomb and 105-mm projectile analysis area. Table 8 lists the parameters and root mean squared error (RMSE) for these two models. The RMSE value represents how well the functional model matches the empirical data points. The lower the RMSE, the more closely the model fits the empirical data. As shown in Table 8, the manually-fit model provides a 37 percent reduction in the RMSE when compared to the automatically-fit model. This is a clear indication that the manually-fit model more closely honors the empirical data points than the automatically-fit model, and that with a small amount of user intervention the variogram model can be significantly improved with corresponding improvements in the resulting kriging estimates.

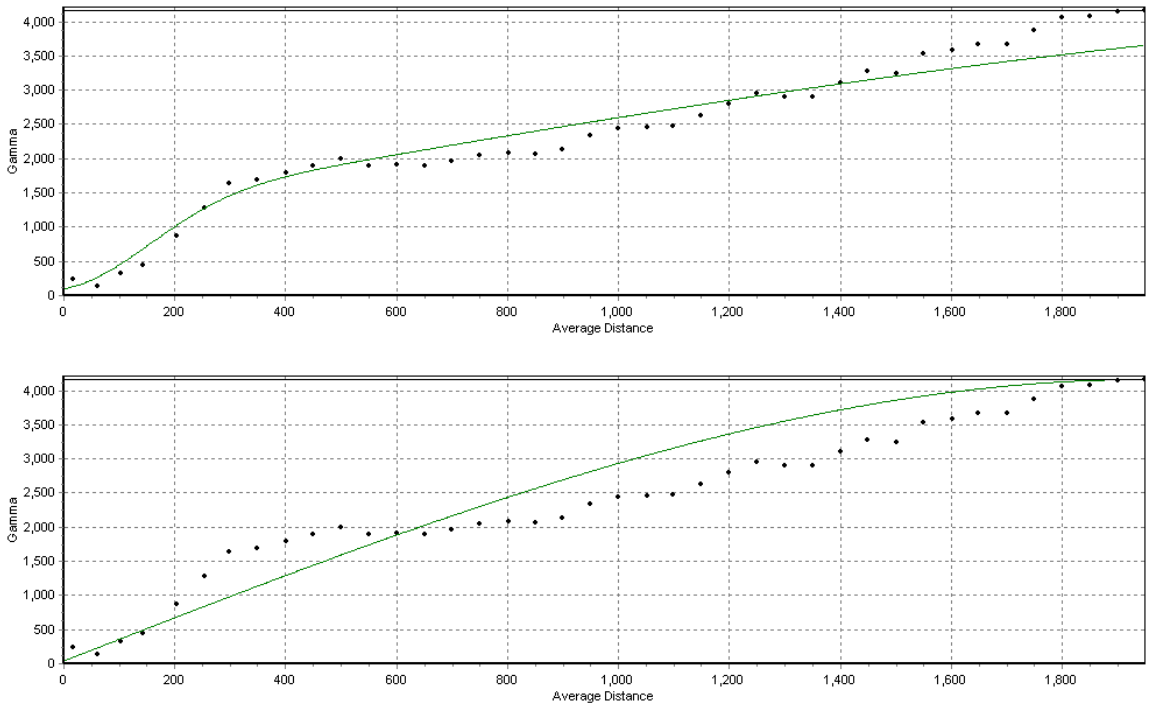

Figure 32. Variogram data and models for the combined 100-lb and 105-mm projectile analysis area used in the sensitivity analysis. The top plot shows the manually-fit model; the bottom plot shows the automatically-fit model. The black dots represent empirical variogram data; the green line shows the functional model used in the kriging.

Table 8. Variogram model parameters and RMSE values for the combined 100-lb and 105-mm projectile analysis area.

Model Fit	RMSE	Nugget	Model	Sill	Range (m)
Automatic	70.9	42	Spherical	4,122	1948
Manual	44.5	100	Spherical	3,000	3,100
			Gaussian	1,100	660

Figure 33 shows the absolute and proportional differences between the kriging anomaly density estimates computed using the automatically-fit variogram and the manually-fit variogram model. The top plot in Figure 33 shows the absolute difference in the kriging results computed with the two different variogram models. These values were computed using the following relationship:

$$\Delta_a(u) = Z_A^*(u) - Z_M^*(u),$$

where $\Delta_a(u)$ is the absolute difference and $Z_A^*(u)$, and $Z_M^*(u)$ are the kriging estimates of anomaly density using the automatically-fit and manually-fit variograms, respectively. The lower plot of Figure 33 shows the proportional difference between the kriging results. The proportional difference, $\Delta_p(u)$, is defined as:

$$\Delta_p(u) = (Z_A^*(u) - Z_M^*(u)) / Z_M^*(u),$$

and scales the difference according to the manual variogram kriging results.

As shown by the plot of absolute differences (top plot of Figure 33), a majority of the area has differences in the kriging results on the order of 1 ApA. The largest differences occur within the higher density areas (denoted by blue lines) and in areas removed from the sampling transects. The proportional difference plot (bottom plot of Figure 33) shows that a vast majority of the area has differences in the kriging results of less then 10 percent. The closeness in the kriging estimates using the two variogram models also is demonstrated in Figure 34, which is a cross-plot of the manually-fit (X axis) and automatically-fit (Y axis) variogram models. A majority of the points in Figure 34 plot are very close to the X = Y line, indicating the results from the two kriging estimates for the combined 100-lb bomb and 105-mm projectile analysis area are very similar.

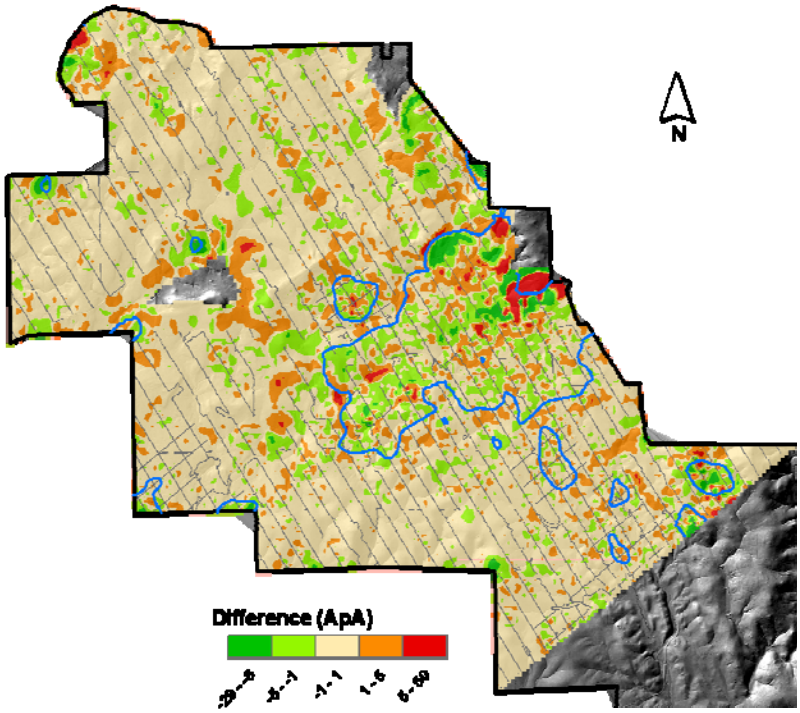

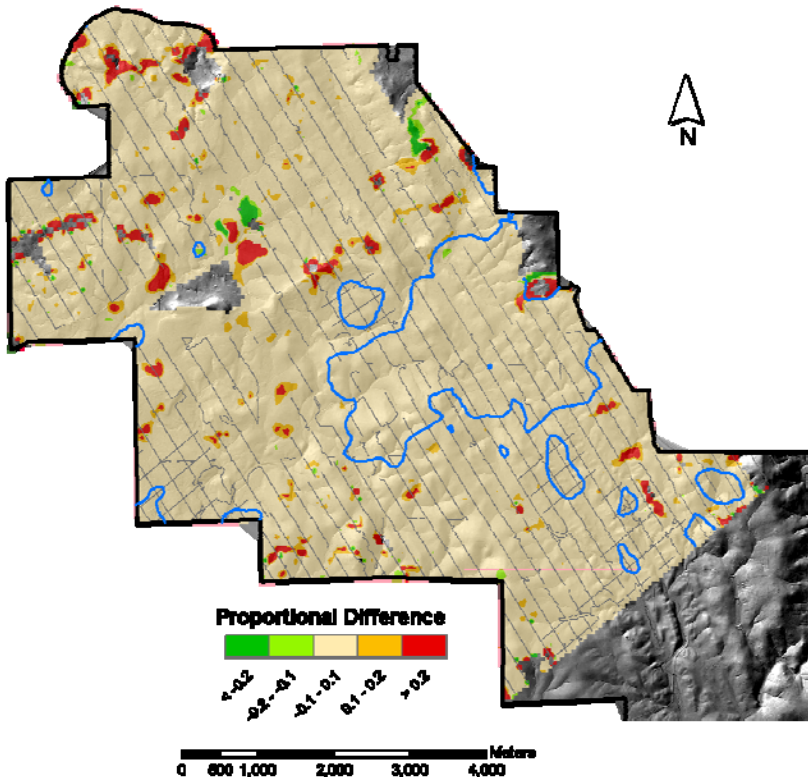

Figure 33. Absolute (top) and proportional (bottom) differences between kriging estimates of anomaly density computed using automatic and manually-fit variogram models for the combined 100-lb and 105-mm projectile analysis area. The blue line, shown for reference, denotes the 95-ApA contour in the manually-fit variogram kriging results.

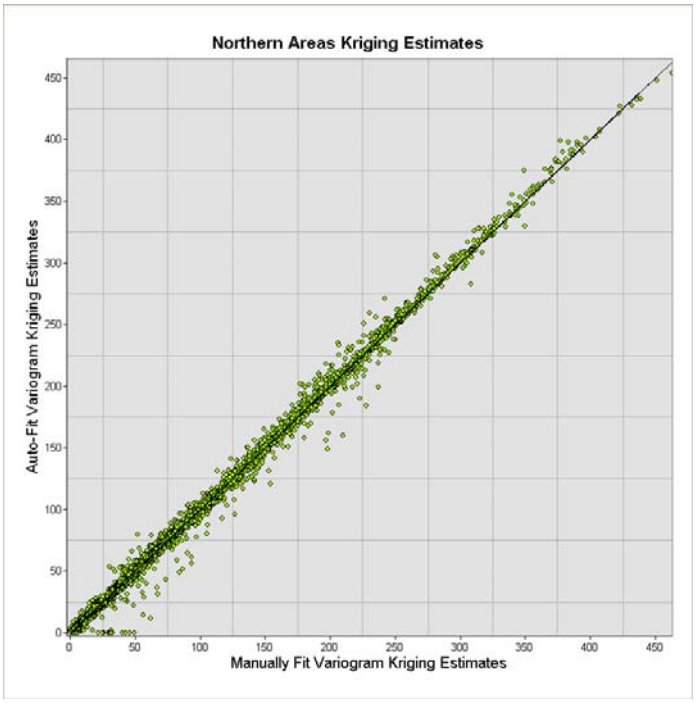

Figure 34. Cross-plot of kriging density estimates for the combined 100-lb bomb and 105-mm projectile analysis area.

In a fashion similar to that applied to the combined 100-lb bomb and 105-mm projectile analysis area, a variogram model sensitivity analysis was also performed for the 81-mm mortar analysis area. Again, differences in the kriging results when using an automatically-fit variogram model versus those from a manually-fit model were investigated. The two different variogram models used are displayed in Figure 35. The parameters and RMSE values for these models are listed in Table 9.

As shown in Table 9, the manually-fit model provides a 72 percent reduction in the RMSE when compared to the automatically-fit model. This is a clear indication that the manually-fit model more closely reflects the empirical data points, and that with a small amount of user intervention the variogram model can be significantly improved with corresponding improvements in the resulting kriging estimates.

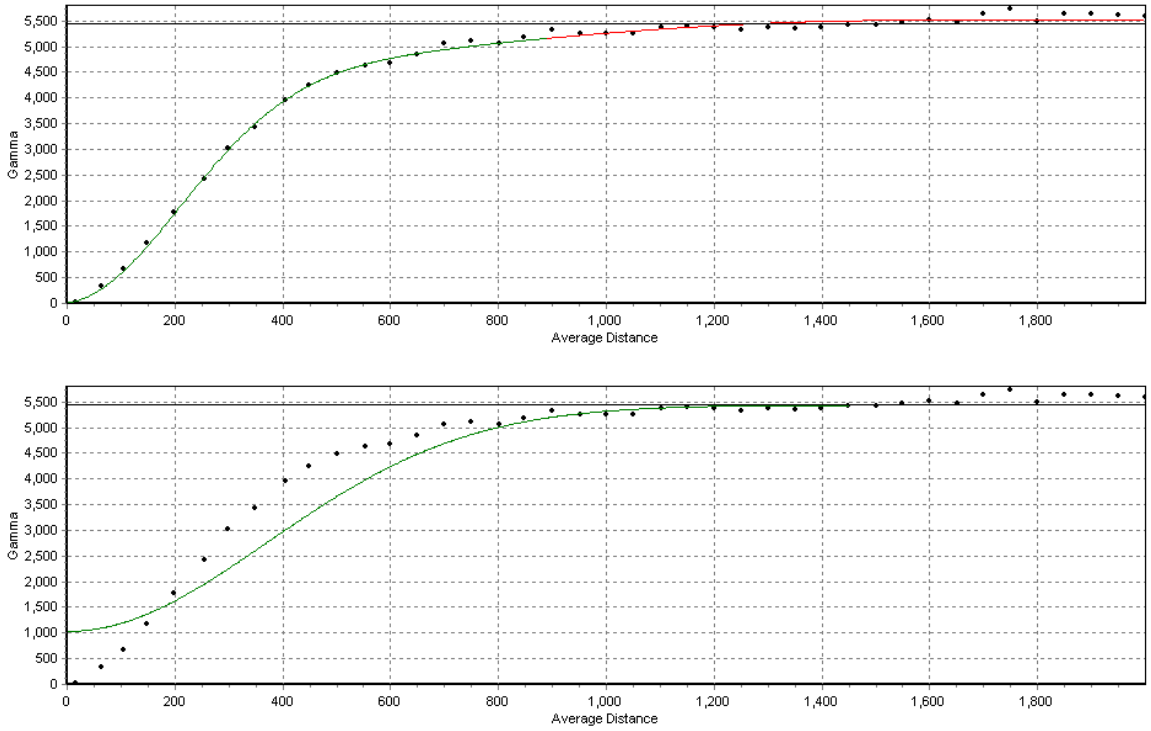

Figure 35. Variogram data and models for the 81-mm mortar analysis area used in the sensitivity analysis. The top plot shows the manually-fit model; the bottom plot shows the automatically-fit model. Black dots represent empirical variogram data; the line that transitions from green to red shows the functional model used in the kriging.

Table 9. Variogram model parameters and RMSE values for the 81-mm mortar analysis area.

Model Fit	RMSE	Nugget	Model	Sill	Range (m)
Automatic	49.5	1,032	Gaussian	4,403	1,574
Manual	13.9	10	Gaussian	4,000	890
			Spherical	1,500	1,550

Figure 36 shows the absolute and proportional differences between the kriging anomaly density estimates computed using the automatically-fit and manually-fit variogram models for the 81-mm mortar analysis area. These differences were computed using the same techniques as those used for the combined 100-lbs and 105-mm projectile analysis area. Note that the absolute difference plot uses a different color scale than that of the other analysis area.

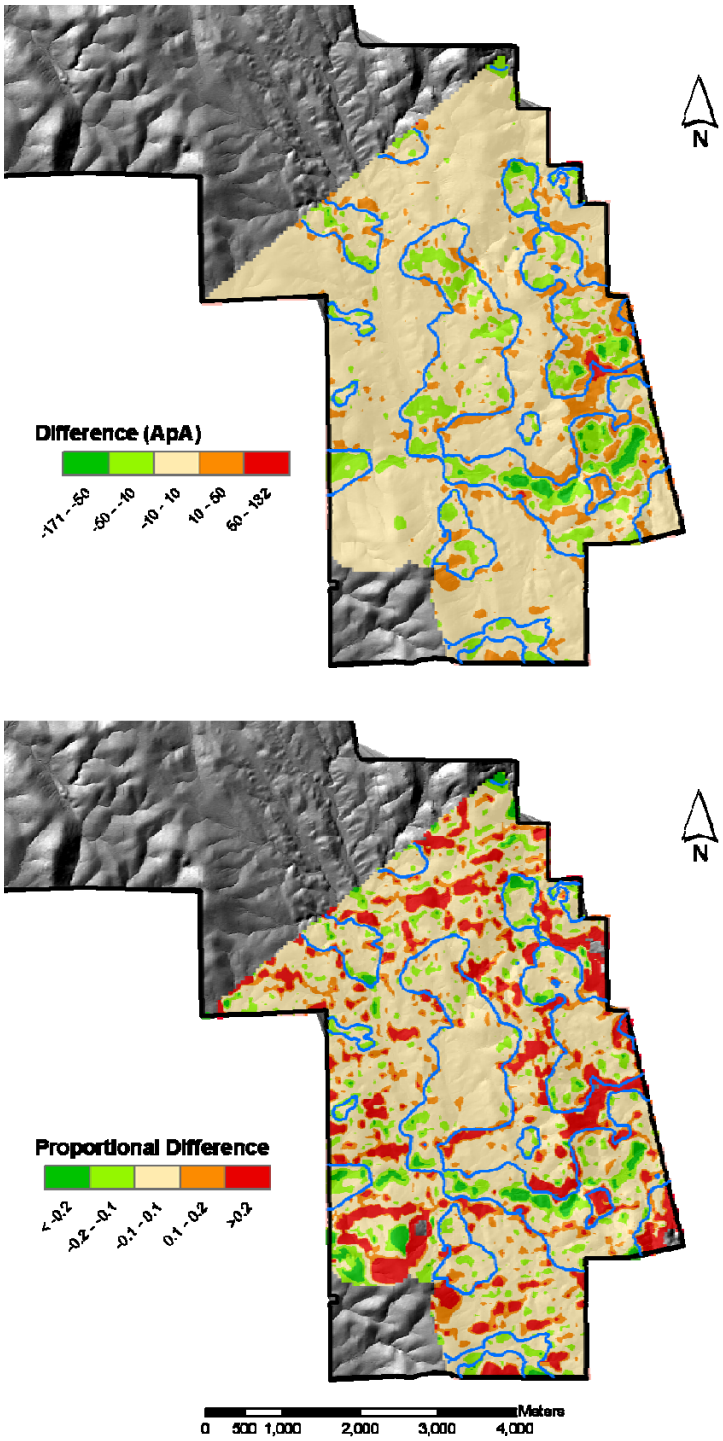

Figure 36. Absolute (top) and proportional (bottom) differences between kriging estimates of anomaly density computed using automatically-fit and manually-fit variogram models for the 81-mm mortar analysis area. The blue line, shown for reference, denotes the 85 ApA contour in the manually-fit variogram kriging results.

In general, the differences in kriging results when using the two different variogram models seen in the 81-mm mortar area are greater than those observed for the combined 100-lb bomb and 105-mm projectile analysis area. As seen in the absolute difference plot of Figure 36, the automatically-fit variogram tends to result in lower anomaly density estimates in the areas with the highest anomaly densities (region inside blue contour line) when compared to the anomaly density estimates generated from the manually-fit variogram model. This difference can also be seen in a cross-plot of the manually-fit and automatically-fit variogram kriging results (Figure 37). In this plot, for the highest density values, the plotted points fall below the X = Y line, indicating that the manually-fit variogram kriging results have higher anomaly density values. Also note that the spread around the X = Y line is much greater in the cross-plot for the 81-mm analysis area (Figure 37) than for the combined 100-lb bomb and 105-mm projectile analysis area (Figure 34).

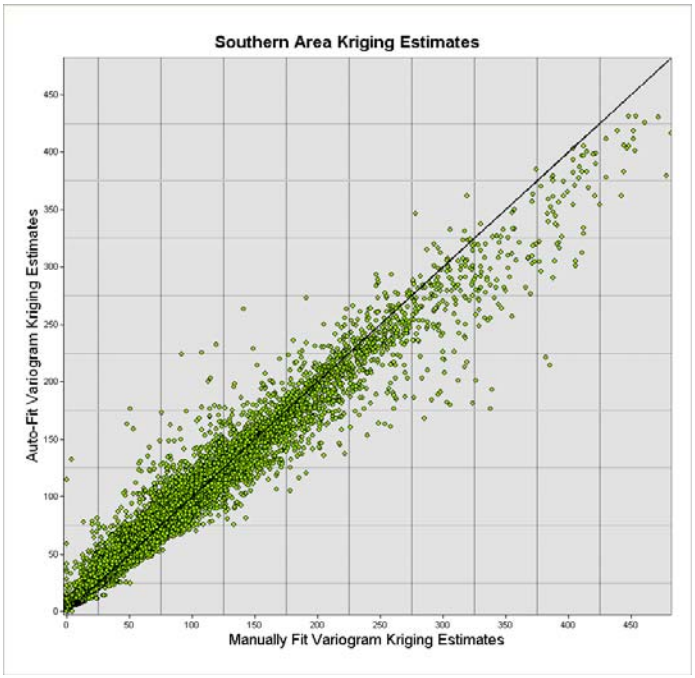

Figure 37. Cross-plot of kriging density estimates for the 81-mm mortar analysis area.

The increased differences for the 81-mm mortar analysis area are likely the result of the larger relative nugget of the automatically-fit variogram model as compared to the nugget used for the manually-fit model (Figure 35). In the automatically-fit variogram model, the nugget is 1032 and the sill is 4403, yielding a relative nugget of 0.23. In the manually-fit model the nugget is 10 and the sill is 5500, yielding a much smaller relative nugget of 0.002. The relative nugget is the ratio of the nugget to the total sill. As the value of a relative nugget increases, the kriging weights are more evenly distributed across the conditioning data (Goovaerts 1997). This would result in a different weighting scheme than was used in the kriging using the manually-fit variogram model and, hence, different anomaly density estimates. For comparison, the nugget ratio for the combined

100-lb bomb and 105-mm projectile analysis area for the automatically-fit and manually-fit variogram models are 0.01 and 0.02, respectively. The kriging results from the automatically-fit and manually-fit variogram models for this area were very similar.

This brief analysis has demonstrated the general level of sensitivity of the kriging results to changes in variogram models for two different regions of the former Camp Beale WAA site. This analysis was not designed to investigate regimented changes in variogram models, rather it was designed to emulate the two different types of models that might be encountered when performing analysis within the VSP UXO module, namely automatically-fit and manually-fit variogram models. This analysis has shown that for the combined 100-lb bomb and 105-mm projectile analysis area, the kriging results from the manually-fit and automatically-fit variogram models are similar. In contrast, the 81-mm mortar analysis area does show large differences between the automatically-fit and manually-fit model kriging results. As discussed above, this likely results from the large differences in nugget values for the two models used in the 81-mm mortar analysis area. This analysis also has demonstrated that with a small amount of user intervention, the variogram models can be significantly improved over those computed automatically. These improvements then should result in corresponding improvements in the subsequent kriging estimates.

3.7. High-Density Area Delineation

The delineation of likely target areas for the Camp Beale WAA site was challenging because the diverse historical uses of the site have resulted in relatively high anomaly densities across large portions of the site. Consequently, while the results here define the most likely target areas, other portions of the site may have been impacted by past munitions use. The areas identified by this study are those that clearly have experienced the greatest impact from past munitions use.

Figure 38 and Figure 39 display the probable target area delineation results for the combined 100-lb bomb/105-mm projectile and the 81-mm mortar analysis areas respectively. In these figures, the anomaly density values are color-coded into three categories. The green-shaded areas represent those regions with the lowest anomaly densities ($\leq$ 50 ApA). Although these areas may have experienced some impact from former munitions use at the site, they are not believed to contain any highly used target areas and can't be distinguished from background. The red-shaded areas represent those regions with the highest anomaly density values. For Figure 38 these are areas with anomaly densities above 95 ApA and for Figure 39 these are areas with densities above 85 ApA. These areas would correspond with those identified in the statistical flagging analysis (section 3.5). These are the areas most likely to contain high-use target areas, and would likely contain the highest percentage of UXO. The yellow-shaded areas represent regions that are transitional between the highest-density and lowest-density areas. These areas may not contain actual target sites, but are likely impacted by munitions use from nearby targets or ranges. The anomaly densities in the yellow-shaded region are not as high as in the red-shaded region, but are still well above the green-shaded region.

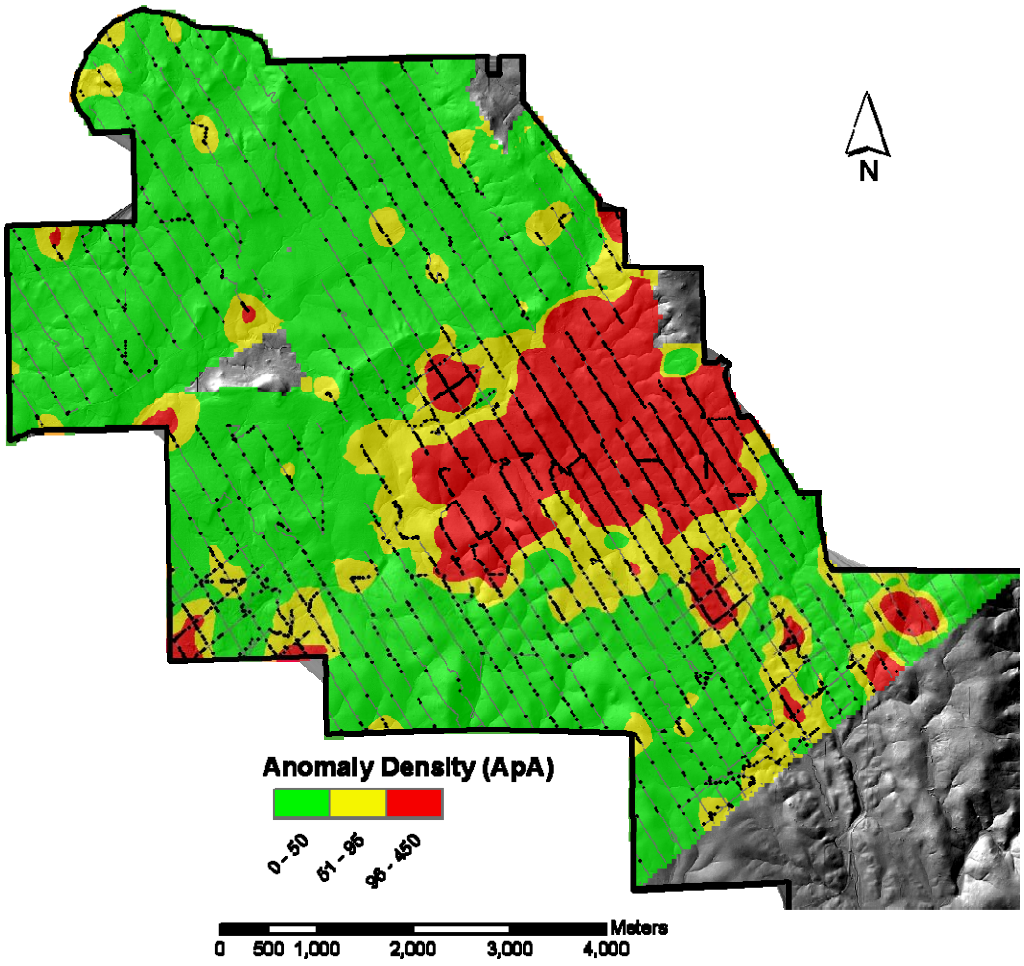

Figure 38. Probable target area delineation for the combined 100-lb bomb and 105-mm projectile analysis area. Color shading indicates the anomaly density range and likelihood of target area location. Red indicates areas most likely to contain target areas; green indicates areas least likely to contain target areas. Yellow regions are transitional zones. Sampling transects and detected anomalies also shown.

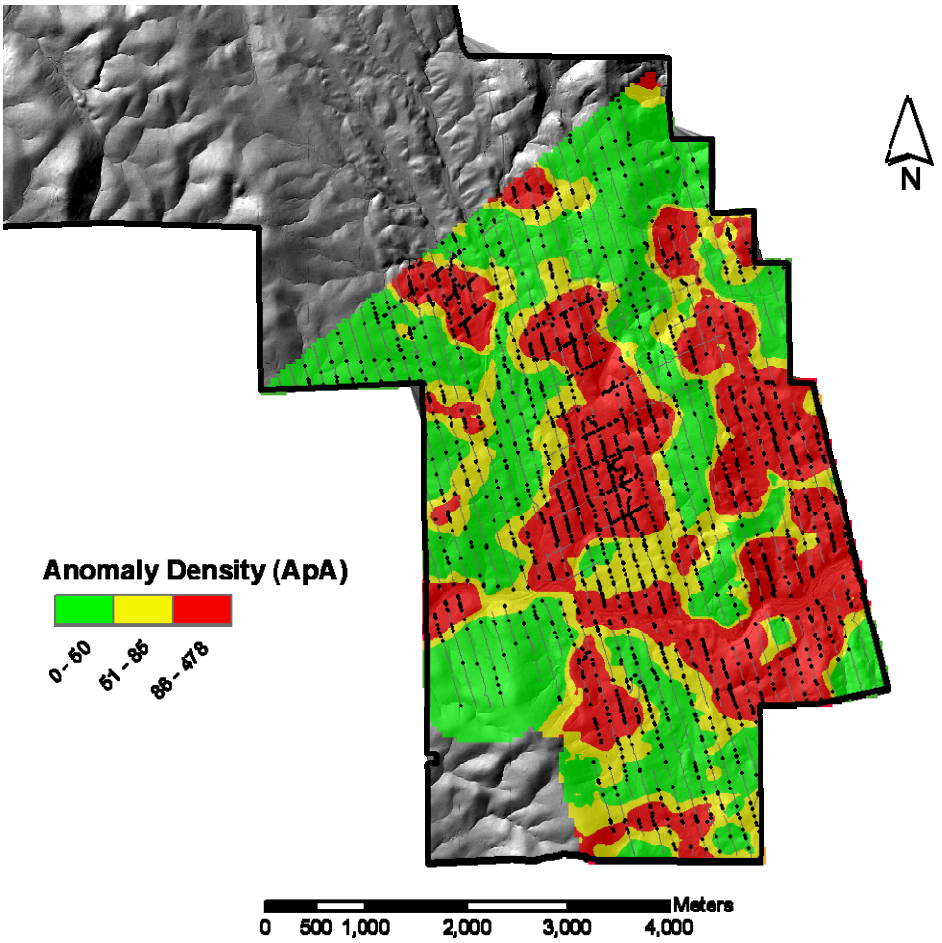

Figure 39. Probable target area delineation for the 81-mm mortar analysis area. Color shading indicates the anomaly density range and likelihood of target area location. Red indicates areas most likely to contain target areas; green indicates areas least likely to contain target areas. Yellow regions are transitional zones. Sampling transects and detected anomalies also are shown.

Table 10 presents the total area and anomaly count as well as the mean anomaly density for each color-zone for the two analysis areas. The 81-mm mortar analysis area, although smaller than the combined 100-lb bomb and 105-mm projectile analysis area, has a larger red-zone area.

Table 10. Areas and total anomaly counts for the three color zones of each analysis area.

Analysis Area	Zone (color)	Area (ac)	Total Anomaly Count	Mean Density (ApA)
Combined 100-lb bomb/ 105-mm projectile	Green	7,716	161,683	21.0
	Yellow	1,943	131,274	67.6
	Red	1,825	311,002	170.4
	Total	11,484	603,959	52.6
81-mm mortar	Green	2,706	76,154	28.1
	Yellow	1,397	91,795	65.7
	Red	2,290	360,979	157.6
	Total	6,393	528,928	82.7

The high percentage of high-density areas, along with the overall higher average densities, indicates that the 81-mm mortar analysis area may have experienced heavier and more widespread munitions use than the combined 100-lbs bomb and 105-mm projectile analysis area. The spatial distributions of high-density locations for the two analysis areas also display different patterns. For the 81-mm mortar analysis area, the high-density areas are broken into a series of medium-size patches that are distributed across the analysis area. Typically, these patches are on the order of 300 to 500 ac in size. In contrast, the combined 100-lb bomb and 105-mm projectile analysis area is dominated by a single large high-density area that covers approximately 1500 ac. This is in addition to several smaller high-density areas on the order of 60 ac in size. One of these smaller areas, located to the north of the large high-density area, is associated with a circular terrain target feature as identified in the lidar survey.

The spatial patterns of high anomaly density would suggest munitions use on a larger area, but in a more concentrated fashion in the combined 100-lb bomb and 105-mm projectile analysis area, and in a more distributed fashion in the 81-mm mortar analysis area. Some overlap between these areas also is evident. The patterns of high anomaly density seen in the two analysis areas are not inconsistent with the information available regarding past munitions use at the former Camp Beale WAA site.[2]

4. Cost Assessment

4.1. Cost Estimates

Estimating costs for this particular technology software is not as straight-forward as estimating costs for survey technologies. There is no cost for obtaining VSP since it is available without charge from the VSP website (http://vsp.pnl.gov). The time cost of using the VSP software is probably minimal compared to the associated time required to gather all the information required to support appropriate selection and input of the VSP parameters.

The major costs involved in using the VSP-UXO modules are associated with the transect design, data analysis, and reporting. As all of these costs are directly related to man hours and the hourly cost of each user is variable, all costs are reported in hours. Table 11 presents some estimated costs to perform an analysis using VSP. There are many hours of time involved in a full wide area assessment and much of this time overlaps with some of the necessary work involved in using VSP. The times reported in Table 11 are an estimate of the time required for VSP related work by a user working on the larger wide area assessment project. It should also be noted that these estimates are not for an

[2] Environmental Security Technology Certification Program (ESTCP). 2006. Wide Area Assessment Pilot Program Demonstration at Former Camp Beale, California. (Unpublished Draft).

expert VSP user. It is anticipated that with experience in VSP the number of hours necessary for a project would decrease.

The estimated costs shown in Table 11 are reported on a per munition region basis as well as those associated with a site similar to camp Beale. For the per region column the costs are based on using one type of survey equipment. The estimated costs reported for the Camp Beale site include the use of two different EM systems with different transect footprints.

Table 11. Cost Model for Visual Sample Plan analysis by a standard user.

Cost Element	Cost Detail	Estimated Costs per Region	Estimated Costs for Camp Beale
Site and Munitions Research Costs	• Archive search report and conceptual site model evaluation • Target area size and shape development	20 hrs	45 hrs
Transect Design Costs	• VSP module use and design finalization • Stake holder interaction	20 hrs	35 hrs
Data Analysis Costs	• Importing anomaly and course-over-ground data • Data evaluation and cleanup • Flagging analysis • Geostatistical analysis	25 hrs	50 hrs
Reporting Costs	• Preliminary report • Detailed final report	30 hrs	50 hrs

4.2. Cost Drivers

The size of the site is not the primary driver for increased costs in the transect design phase. As each region will require a unique transect design and evaluation, the costs will increase based on the number of subdivided munitions regions and survey equipment types.

The data analysis and reporting costs are also affected by the number of subdivided munitions regions and survey equipment types. However, the data analysis and reporting costs can also be affected by the number of unique high density areas, differences between background and target area anomaly densities, the geology, and the terrain.

4.3. Cost Benefit

The benefit of using VSP for sparse transect surveys is realized in the small proportion of the site which needs to be surveyed to obtain reliable results. During most of the demonstrations performed, less than 2% of the site has been surveyed to produce reliable results that identified the appropriate high density areas. As much of the cost associated with wide area assessment is the expense of the survey work, the relatively small amount of time in VSP can produce a very large cost benefit for large sites. Also, having a tool like VSP which automates the evaluations of detection probabilities and facilitates parameter tradeoff studies can save significant time and effort, thereby providing a significant cost benefit.

5. Conclusion

This report has summarized the results obtained from the analysis of geophysical transect sampling of a WAA study site located at the former Camp Beale in California. Statistical and geostatistical analysis of the anomaly density along the sample transects has been used to identify locations with high magnetic anomaly densities. These locations represent areas that experienced the greatest impact from munitions use at the site, and represent the most likely locations of former target areas.

Among the WAA study sites, the former Camp Beale site is unique in its use history. Camp Beale site has a complex history of multiple uses (aerial bombing and artillery firing) and multiple overlapping target areas and firing fans (ESTCP 2006). Because of this unique history, the site has experienced some level of impact from munitions use. This can be seen in the relatively high anomaly densities observed across the site (Figure 38 and Figure 39). This finding is in contrast to the findings for other WAA study sites (i.e., Pueblo Precision Bombing Range, Victorville, etc.) where distinct isolated target features were superimposed on a relatively low background anomaly density (Hathaway et al. 2006, 2007). The result is that for the Camp Beale WAA site, the highest density areas (red zones in Figure 38 and Figure 39) represent the areas with the greatest impact from past munitions use; however, these areas are not necessarily the only ones that may have experienced munitions use.

For the entire former Camp Beale WAA site, the highest density (red-zone) area is 4115 ac in size, with an estimated 671,981 magnetic anomalies falling within this area. The total area covered in the geostatistical analysis for this site was 17,877 ac. Therefore, approximately 23 percent of this WAA site is contained within the highest anomaly density (red) zone (Figure 38 and Figure 39). Approximately 58 percent (10,422 ac) of the site has anomaly densities below 50 ApA (the green-zone), and 19 percent of the site (3340 ac) has anomaly densities that are above 50 ApA but below the highest density threshold (the yellow-zone). The total anomaly count exclusive of the red zone is estimated to be 460,906, bringing the estimated total anomaly count for the entire site to well over 1 million.

6. References

Department of Defense Explosives Safety Board (DDESB). 2003. "Methodologies for Calculating Primary Fragment Characteristics." Technical Paper-16 (TP-16), Alexandria, Virginia.

Goovaerts P. 1997. *Geostatistics for Natural Resources Evaluation*. Applied Geostatistics Series, Oxford University Press, Inc., New York.

Harbaugh GR, DA Steinhurst, and N Khadr. 2006. *Wide Area UXO Contamination Evaluation by Transect Magnetometer Surveys, Pueblo Precision Bombing and Pattern Gunnery Range #2*. NOVA-2031-TR-0001, Nova, Washington, D.C.

Harbaugh GR, and DA Steinhurst. 2007. *Wide Area UXO Contamination Evaluation by Transect Magnetometer Surveys, Man-Portable EM Demonstration Data Report, Victorville Precision Bombing Ranges Y and 1.* NOVA-2031-TR-0003, Nova, Washington, D.C.

Hathaway J, BL Roberts, SA McKenna, and BA Pulsipher. 2006. *Application of Statistically-Based Site Characterization Tools to the Victorville Precision Bombing Range Y and 15 for the ESTCP Wide Area Assessment Demonstration*. PNNL-16138, Pacific Northwest National Laboratory, Richland, Washington.

Hathaway J, BL Roberts, SA McKenna, and BA Pulsipher. 2007. *Application of Statistically-Based Site Characterization Tools to the Pueblo Precision Bombing and Pattern Gunnery Range #2 for the ESTCP Wide Area Assessment Demonstration*. PNNL-16418, Pacific Northwest National Laboratory, Richland, Washington.

Hathaway JE, BL Roberts, SA McKenna, and BA Pulsipher. 2008. *Using the VSP-UXO Modules to Support Site Characterization*. PNNL-17382, Pacific Northwest National Laboratory, Richland, Washington.

Matzke BD, NL Hassig, JE Wilson, RO Gilbert, BA Pulsipher, LL Nuffer, ST Dowson, J Hathaway, CJ Murray, and LH Sego. 2007. *Visual Sample Plan Version 5.0 User's Guide*. PNNL-16939, Pacific Northwest National Laboratory, Richland, Washington.

Roberts BL, J Hathaway, SA McKenna, and BA Pulsipher. 2007. *Application of Statistically-Based Characterization Tools to the Former Erie Army Depot and Toussaint River Site for the ESTCP Wide Area Assessment Demonstration*. PNNL-16550, Pacific Northwest National Laboratory, Richland, Washington.